Anja Kjærnes Eilertsen

DC Breakdown Strength of HVDC XLPE Cable Insulation

Short-term testing of cable peelings

Master's thesis in Energy and Environmental Engineering
Supervisor: Frank Mauseth
Co-supervisor: Espen Doedens
June 2023

Master's thesis

NTNU
Norwegian University of Science and Technology
Faculty of Information Technology and Electrical Engineering
Department of Electric Power Engineering

NTNU
Norwegian University of
Science and Technology

Anja Kjærnes Eilertsen

DC Breakdown Strength of HVDC XLPE Cable Insulation

Short-term testing of cable peelings

Master's thesis in Energy and Environmental Engineering
Supervisor: Frank Mauseth
Co-supervisor: Espen Doedens
June 2023

Norwegian University of Science and Technology
Faculty of Information Technology and Electrical Engineering
Department of Electric Power Engineering

NTNU
Norwegian University of
Science and Technology

Preface

This Master's thesis is the final project of the two-year Master's degree program Energy and the Environment, carried out at the Norwegian University of Science and Technology (NTNU) in Trondheim in the spring of 2023.

The scope of the work has been to investigate to what degree the short-time DC electrical breakdown strength of XLPE insulation of HVDC cables changes as the material ages.

I want to thank my supervisor, associate professor Frank Mauseth at NTNU, for always being available for questions and helping with the experimental work at the lab.

I am also thankful to my co-supervisor, Espen Doedens in Nexans, for lots of advice and for sharing his experiences around DC breakdown testing, considering test setup, procedure, and the theoretical aspect.

I am grateful for NTNU's mechanical and electrical workshop. Thanks to Morten Flå for the construction of the test cell and part of the test setup and for providing me with additional equipment for testing. I would also give an extra thanks to Bård Almås and Anyuan Chen for all their help at the lab.

Lastly, I would like to thank my family for support, and all my friends in Trondheim for giving me five unforgettable years.

Trondheim, June 12^{th} 2023

Anja Kjærnes Eilertsen

Anja Kjærnes Eilertsen

Abstract

In the electrification of society, leading to higher total electricity demand and the aim for sustainable solutions, extruded high voltage direct current (HVDC) cables are a key factor. Concerning renewable energy sources, HVDC cables are essential, for instance, as links between land and offshore wind parks. The use of extruded 525 kV HVDC cables are increasing, and designs for even higher voltage levels are in development. Consequently, it is an increased interest in understanding how crosslinked polyethylene (XLPE) ages under thermo-electrical stress. Aging behavior is crucial, considering the reliability of high voltage transmission systems.

This study aims to investigate to what degree the short-time DC electrical breakdown strength of XLPE insulation of HVDC cables changes as the material ages. To investigate this, short-term breakdown tests under the application of DC voltage are performed on XLPE in the form of cable peeling. The cable peeling was cut from the outer semiconductor to the inner semiconductor from a full-scale 525 kV HVDC cable. One of the test samples was fresh (unaged) XLPE insulation. The other was exposed to prequalification (PQ) tests which aim to correspond with 40 years of thermo-electrical aging. In addition, it was desired to investigate if the breakdown strength is affected by the radial position in the insulation.

The DC breakdown tests were performed using a DC source and a test cell established in a preliminary study. The circuit also provided the ability for secure measurement of the breakdown voltage. The cable peeling was sandwiched between two electrodes, and the voltage was increased in steps of 1 kV per minute until breakdown occurred. For each cable peeling, a series of 20 tests were conducted on three regions; insulation close to the inner semiconductor, middle insulation, and insulation close to the outer semiconductor. The thickness of the breakdown channels was measured, and the DC breakdown strengths were determined in kV/mm. All data were treated using 2-parameter Weibull distribution.

From the DC breakdown tests performed on the fresh insulation, the 63.2% characteristic breakdown strengths were in the range of 550-580 kV/mm for the three regions of the insulation. For the aged insulation, the breakdown strengths were in the range of approximately 380-400 kV/mm. It was seen no statistically significant difference in the breakdown strength of the regions in either of the insulation specimens. Due to no significant difference, the conclusion is that the DC breakdown strength of XLPE is not dependent on the radial position of the cable insulation.

The fresh insulation tested in this project shows higher breakdown strength than the results from previous studies conducted on the DC breakdown strength of XLPE cable peeling. The 63.2% characteristic breakdown strength is over 100 kV/mm greater than in the previous studies. Possible volume effects are minor, suggesting that the higher breakdown strengths indicate a better XLPE matrix of the tested insulation in this project than the previously tested insulation.

When comparing the 63.2% characteristic breakdown strength of the aged insulation with the fresh, the breakdown strength has been reduced by over 150 kV/mm. Consequently, the reduction is 30% in breakdown strength for all regions. A reduction of 30% after 40 years of thermo-electrical stress suggests a longer residual lifetime. The findings in this work indicate that an expectation of 40 years of lifetime for this type of HVDC cable can be considered conservative.

Keywords: HVDC cable, cable peeling, XLPE, electrical breakdown strength, aging, short-term testing

Sammendrag

I sammenheng med elektrifisering av dagens samfunn, som fører til høyere elektrisitetsbehov og et mål om bærekraftige løsninger, er ekstruderte høyspennings-likestrømskabler (HVDC-kabel) en nøkkelfaktor. HVDC-kabler er essensielle når det gjelder fornybare energikilder, for eksempel som forbindelse mellom land og offshore vindparker. Bruken av ekstruderte 525 kV HVDC-kabler øker, og design for enda høyere merksespenning er i utvikling. Dette medfører interesse for å forstå hvordan kryssbundet polyethylene (PEX) aldres under termo-elektrisk stress. Hvordan aldringen av en HVDC-kabel påvirkes er avgjørende for påliteligheten til høyspente overføringssystemer.

Målet med dette studiet er å undersøke i hvilken grad elektrisk holdfasthetsstyrke til PEX endres ved aldring av materialet, under påtrykk av likespenning (DC). For å undersøke dette har det blitt gjennomført korttids-holdfasthetstester på PEX i form av kabelpeeling. Kabelpeelingen ble kuttet fra ytre halvleder til indre halvleder fra en full-skala 525 kV HVDC-kabel. En av prøveobjektene var ualdret PEX isolasjon. Den andre var PEX isolasjon som har vært gjennom prekvalifiserings (PQ) test som skal tilsvare 40 år med termo-elektrisk aldring. I tillegg var det ønskelig å undersøke om holdfasthetsstyrken påvirkes av radiell posisjon i isolasjonen.

Gjennomslagstestene ble utført ved bruk av en elektrisk krets som genererte stabil DC spenning og en testecelle som ble laget i forprosjektet til masteroppgaven. Kretsen ga også mulighet for sikker måling av gjennomslagspenningen. Kabelpeelingen ble klemt mellom to elektroder og spenningen ble økt med steg på 1 kV per minutt til gjennomsalg. På hver kabelpeeling ble det gjennomført 20 tester for hver region i isolasjonen; isolasjon nær indre halvleder, midtre isolasjon og isolasjon nær ytre halvleder. Tykkelsen på gjennomslagskanelene ble målt, og holdfasthetsstyrken i kV/mm ble beregnet. Dataen ble behandlet med 2-parameter Weibullfordeling.

Gjennomslagstestene gjennomført på ualdret isolasjon ga en 63,2% karakteristisk holdfasthetsstyrke mellom 550-580 kV/mm for de tre regionene av isolasjonen. For aldret isolasjon var holdfasthetsstyrken mellom 380-400 kV/mm. Det ble ikke sett en statistisk signifikant forskjell i holdfasthetsstyrken til regionene for prøveobjektene. På grunn av ingen signifikant forskjell konkluderes det med at holdfasthetsstyrken til PEX under påtrykk av DC ikke er avhengig av radiell posisjon i isolasjonen.

Den ualdrede isolasjonen testet i dette prosjektet viser høyere korttids-holdfasthetsstyrke enn resultatene fra tidligere studier på holdfasthetsstyrken til PEX kabelpeeling under påtrykk av DC. Basert på 63,2% karakteristisk holdfasthetsstyrke, er styrken over 100 kV/mm bedre sammenlignet med tidligere studier. Hvis man ser bort ifra mulig påvirknig fra volum, kan den høyere holdfasthetsstyrken indikere at material-sammensetningen for PEX isolasjonen testet i dette prosjektet er bedre en tidligere testet isolasjon.

Ved sammenligning mellom 63,2% karakteristisk holdfasthetsstyrke til den aldrede og ualdrede isolasjonen, har styrken blitt redusert over 150 kV/mm. Følgende er reduksjon i holdfasthetsstyrke på 30% for alle regioner. En reduksjon på 30% etter 40 år med termo-elektrisk stress kan tyde på lengre restlevetid. Funnene i dette arbeidet gir indikasjon på at forventet levetid på 40 år for denne typen HVDC-kabler, er å anse som konservativ.

Abbreviations

AC	Alternating Current
CI	Confidence interval
DC	Direct Current
HV	High Voltage
LV	Low Voltage
MI	Mass impregnated
PD	Partial Discharge
PQ test	Prequalification test
RMS	Root mean square
Variac	Variable AC Power Supply
XLPE	Crosslinked Polyethylene

Table of Contents

List of Figures **ix**

List of Tables **x**

1 Introduction **1**

1.1 Background 1

1.2 Scope of thesis 3

2 Theory **4**

2.1 Crosslinked Polyethylene as a solid dielectric 4

2.2 Aging and degradation of crosslinked polyethylene 5

2.2.1 Electrical aging 5

2.2.2 Chemical aging 6

2.2.3 Physical aging 6

2.3 Charge injection and charge transport 6

2.4 Electrical breakdown in solid dielectrics 7

2.5 Prequalification Tests 8

2.6 Dielectric Breakdown testing 9

2.6.1 The stochastic behavior of electrical breakdown 9

2.6.2 Challenges with destructive tests on solid dielectrics 10

2.7 State of the art of DC breakdown testing on XLPE insulation 11

3 Experimental work **14**

3.1 The Test setup 14

3.1.1 Electrodes 17

3.1.2 The Test cell 18

3.2 The Test object 19

3.2.1 Preparation before testing 20

3.3 Collecting data of DC breakdown strength 21

3.3.1 The applied DC voltage 21

3.3.2 Circumstances of measurements 22

3.3.3 Procedure for measurements 23

4 Results and Discussion **26**

4.1 The DC breakdown strength of aged XLPE cable peeling 27

4.2 The DC breakdown strength of fresh XLPE cable peeling 30

4.3 Comparison: DC Breakdown strength of Fresh vs. Aged XLPE cable peeling . . 33

4.4 Possible errors/limitations in measurements 36

4.4.1 Handling/preparation of the test objects 36

4.4.2 Thickness of the cable peeling 37

4.4.3 Automatic Voltage adjustment 37

4.4.4 Pitting on electrodes 38

4.5 Anchoring the DC breakdown strength values to an actual HVDC cable 38

5 Conclusion **39**

6 Suggestions for further work **40**

Bibliography **41**

Appendix **44**

A List of Equipment **44**

B DC breakdown data - Aged XLPE cable peeling **45**

C DC breakdown data - Fresh XLPE cable peeling **48**

List of Figures

1.1 The United Nations approach on a sustainable development regarding the environment and industry 1

1.2 General structure of a single core cable 2

2.1 The difference in structure between polyethylene and crosslinked polyethylene . . 4

2.2 Bathtub curve 9

3.1 Electric circuit used for DC breakdown testing 14

3.2 Setup for automatic adjustment of applied voltage 15

3.3 The electrodes in the test cell 17
3.4 The test cell 18
3.5 The test object: cable peeling 19
3.6 Orientation within the cable peeling 20
3.7 The AC signal and corresponding applied DC signal 21
3.8 Basic illustration of the DC step voltage applied to the test object until breakdown 24
3.9 Micrometer used for thickness measurements 25
4.1 Weibull probability plot of the DC breakdown strength of the aged XLPE insulation 27
4.2 Weibull probability plot of the DC breakdown strength of the fresh XLPE insulation 30
4.3 Breakdown channels from the fresh cable peeling. 32
4.4 Bar chart comparing the 63.2% characteristic breakdown strength of the fresh and aged XLPE cable peeling 33

List of Tables

2.1 Factors causing aging of cable insulating systems 5
2.2 *State of the art* - The obtained scale and shape parameter for the DC breakdown tests 12
2.3 *State of the art* - The obtained scale and shape parameter for the DC breakdown tests performed at 30°C 13
3.1 Settings in LabVIEW 23
3.2 The series of the DC breakdown testing 24
4.1 Scale and shape parameter of the Weibull distribution for the three test series performed on aged XLPE insulation 27
4.2 Scale and shape parameters of the Weibull distribution for the three test series performed on aged XLPE insulation 30
4.3 Reduction of the 63.2% breakdown strength considering the fresh and aged insulation specimens 34
4.4 The shape values for the different regions of fresh and aged insulation specimens 34
A.1 Equipment used in the experimental work 44
B.1 The DC breakdown data obtained for the outer XLPE of the aged specimen . . . 45
B.2 The DC breakdown data obtained for the middle XLPE of the aged specimen . . 46
B.3 The DC breakdown data obtained for the inner XLPE of the aged specimen . . . 47
C.1 The DC breakdown data obtained for the outer XLPE of the fresh specimen . . . 48

C.2 The DC breakdown data obtained for the middle XLPE of the fresh specimen . . . 49
C.3 The DC breakdown data obtained for the inner XLPE of the fresh specimen . . . 50

1 Introduction

This thesis builds upon the preliminary work done in the Specialization project in the course TET4510 Electrical Energy and Power Systems, delivered at NTNU in December 2022 [1]. Therefore, the content in the background for this thesis is similar to the background for the Specialization project. The paragraphs on cable design and the final paragraph in subsection 1.1 are taken from the Specialization project, involving corrections.

1.1 Background

As a result of our developing society, where electrification is being highly prioritized nowadays, the desire for development within high voltage (HV) transmission systems also increases. The present high energy consumption levels and the future extension of habitation and industry will generally require more electricity. The requirement will lead to an even higher total electricity demand in society. Not only is a large amount of energy needed, but it is also a demand for enabling the transfer of energy over even longer distances [2].

Due to renewable source intermittency and remoteness to urban areas, the possibility of transferring a high amount of energy over long distances is highly relevant in the green transition. For instance, subsea cables are used in projects involving offshore wind power. They are also used to connect countries and transfer energy from countries with renewable energy sources to countries with only fossil fuels. Both the European Commission and the United Nations have agendas where development within the energy sector is relevant. The European Green Deal, delivered in 2019, has the aim to "*make Europe climate neutral by 2050, boost the economy through green technology, create sustainable industry and transport, and cut pollution*" [3, 4]. Obtaining solutions that both cover the energy demand from society and, at the same time, are sustainable is crucial for Europe to achieve these goals. The United Nations have 17 sustainable development goals. Three of these goals can be associated with preserving the environment through the electrification of society. Figure 1.1a, 1.1b and 1.1c show the three relevant goals.

(a) Goal 7: "*Affordable and clean energy*"

(b) Goal 9: "*Industry, innovation and infrastructure*"

(c) Goal 13: "*Climate action*"

Figure 1.1: United Nations approach on a sustainable development regarding the environment and industry. All three figures can be found in reference [5].

Goal number 7 involves interaction between countries to share renewable energy sources and develop the electrical grid to ensure the security of supply. Goal number 13 is also dependent on the use of renewable energy sources and cut the use of fossil fuels. Considering goal number 13, it is no direct connection to the environment. The goal can be associated with the environment as the focus is the development of industry, where the electrification of society plays an important role.

The desire to transport a high amount of energy over even longer distances requires a lot from the power transmission system, which couples the power grid together. For energy companies which distribute electricity, the security of supply is fundamental, and the chosen solutions should be as cost-effective and reliable as possible. As the amount of power to transfer increases, increasing the rated voltage level for power cables and overhead power lines is also desired, as this will minimize power losses. High voltage direct current (HVDC) transmission systems are a frequently used solution considering large-capacity transmission over long distances [6].

HVDC transmission systems are beneficial over high voltage alternating current (HVAC) transmission systems due to the limitations AC systems entail [6]. Even though DC-AC converter stations are necessary to utilize HVDC transmission systems in the power grid, which involves higher costs and losses, HVDC is advantageous over HVAC beyond the break-even distance. Above the break-even distance, an HVAC transmission system's cost will be higher than an HVDC transmission system's [7, 8]. The reason for this is factors like charging current, skin effect, and necessary reactive compensation systems related to AC [6, 8]. The last few years have seen increased usage of HVDC cable systems with crosslinked polyethylene (XLPE) as insulation material [9]. The increased use is based on several factors. Such cable systems have high reliability and superior electrical performances relative to mass impregnated (MI) cables. They are lightweight, the maintenance is undemanding, and they are environmentally friendly [6].

The design of cables used in HV applications varies a lot, and is dependent on different factors. All individual projects have cables with design parameters chosen to optimize the product based on specifications in the project. Power cables consists of several layers where each layer has its own purpose. Standard cable configuration is either single-core or three-core [8]. One layer that is always present in a cable configuration is the insulation layer. There are different types of insulation systems. The main types are MI cables and extruded polymers; such as XLPE [10]. A general structure of an single core cable is shown in Figure 1.2. Both the material for the layers and the number of layers within a cable configuration will vary [8].

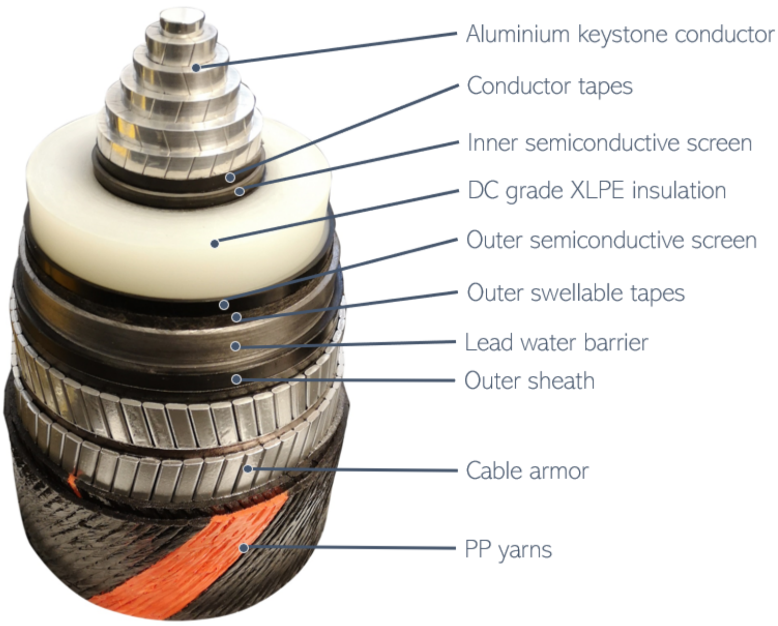

Figure 1.2: General structure of a single core cable. The picture is of an HVDC cable, provided by Nexans Norway AS.

Considering the transfer of energy at a higher voltage level, the stresses in the electrical insulation system will be higher. To ensure a reliable power supply, it is necessary to know how different parts of the complex power system will be affected. This leads to an aim for understanding the lifetime of extruded HV cables, especially HVDC cables [11]. It is crucial to obtain information about the long term thermo-electrical aging behavior of insulation as the thermal and electric profile are the main factors considering the function of the power cable [12]. A better understanding of aging allows for designing cable systems with better performance and sustainability. This makes it relevant to collect data on withstand the strength of the dielectric, which can be done by breakdown testing. Considering HV cable systems, more research has been performed on the influence of AC application on XLPE than an application of DC. However, throughout the years, analysis concerning the effect of HVDC has increased [9].

1.2 Scope of thesis

This thesis aims to investigate to what degree the electrical properties in the insulation layer of HVDC cables change as the material ages. It is desired to collect data on the breakdown strength of XLPE cable insulation under the application of DC voltage and subsequently perform a statistical analysis of the data. To collect enough data so that the amount of data is of a considerable size, enough test samples that are as identical as possible are essential. Therefore, the idea is to obtain XLPE insulation in the form of cable peeling, cut from an actual HVDC cable, which has been manufactured following the typical processes. The cable peeling tested is cut from a full-scale cable end from a cable produced by Nexans Norway AS.

The breakdown tests are performed on the cable peeling. It is desired to obtain breakdown data from different parts of the insulation to investigate possible differences. Hence, the testing per individual cable peeling sample is done in three series. Each series correspond with an area in the cable insulation:

- Near the inner semiconductor
- Middle of insulation
- Near the outer semiconductor

Comparing how different energizing patterns may change the breakdown strength of XLPE is desired. The idea is to obtain DC breakdown data from pristine, 'fresh' XLPE cable insulation and from XLPE insulation collected from a cable that has been through prequalification (PQ) tests.

The experimental work done in this project aims to assess how the condition of the insulation is before and after PQ tests, thus to what degree it changes as the insulation ages. Furthermore, the work contributes to investigating how DC affects polymeric insulating materials.

2 Theory

2.1 Crosslinked Polyethylene as a solid dielectric

Throughout the years, the advancement of XLPE materials has enabled possibilities for such cables to be used in applications with increasing voltage levels. XLPE is a thermosetting material made by crosslinking the thermoplastic material polyethylene (PE). The crosslinking is often done using chemical curing processes such as vulcanization [13]. XLPE (and PE) are polymers often used as insulation material in electrical components, thus categorized as solid dielectrics. A polymer is a material built up by monomers linked together during polymerization that results in long, organic chain molecules [14]. Polymers, as non-conductive materials, are chemically saturated structures resulting in good electric properties of the material. In saturated structures, the electrons between the atoms are solid-bounded, so no free electrons will be available for carrying an electric current. Another factor making polymers a good option for insulation is the possibility for molding and shaping [15].

In the production run of a cable, the polymer can be extruded over the conductor using extruders where there must be a certain temperature[16]. In this process, the material is shaped. After extrusion, the vulcanization process establishes crosslinks between the PE chains, and the linear segments are changed to a three-dimensional network [14]. The control of the triple-extrusion process has been developed throughout the years. The resulting quality of the insulation is high, as the presence of void and contaminants is lowered [17]. Figure 2.1a and 2.1b show the molecular structure and a schematic presentation of PE and XLPE, respectively [18].

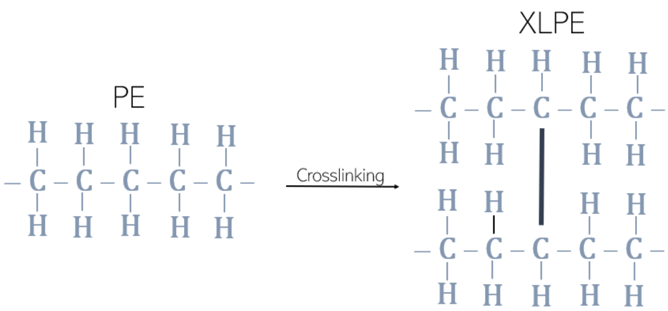

(a) The molecular structure of PE and XLPE.

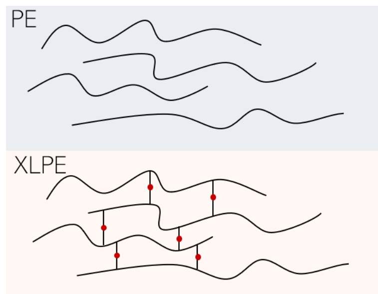

(b) Schematic presentation of PE and XLPE. The figure is inspired by Figure 5 in reference [19].

Figure 2.1: The difference in structure between polyethylene and crosslinked polyethylene [18].

In Figure 2.1a, the difference between the molecular structure of PE and XLPE is seen, while in the schematic presentation, there are bondings between several PE chains, resulting in a complex, three-dimensional network. In the extrusion and vulcanization process, the subsequent cooling will highly impact the crystallization of the polymer [14]. The crystallinity of XLPE will vary as both crystalline and amorphous regions are present, resulting in a semi-crystalline structure [20]. Furthermore, the crystallization will affect the morphology and structure of the material. Concerning this, the degree of crystallinity will affect the electrical and mechanical properties of the material [14]. Another factor contributing to the behavior of XLPE is the degree of crosslinking. By crosslinking PE, the material gets stronger as thermal and mechanical properties improve, and the material gets more chemically stable. Thus, the material's performance is improved [11, 16].

2.2 Aging and degradation of crosslinked polyethylene

All components in the electrical power system are exposed to a variety of stresses. The stress will lead to aging of the insulation, where the aging can be a result of factors based on processes in the material itself (intrinsic aging) or due to external factors (extrinsic aging) [11]. External factors causing aging can be elements like contaminants and physical defects, which can arise under manufacturing, transport, installation, etc. Such defects can, for instance, be voids developed under the extrusion process [21]. For power systems, the stresses can be electrical, mechanical, thermal, and environmental [22]. More specific aging mechanisms for power cables are listed in the four divisions in Table 2.1 [21].

Table 2.1: Factors causing aging of cable insulating systems [21].

Electrical	**Mechanical**	**Thermal**	**Environmental**
Voltage Current Frequency	Tensions Bending Vibrations Compression Torsion	Maximum temperature Ambient temperature Temperature gradient Temperature cycling Radiation	Water/humidity Corrosive chemicals Gases Lubricants

A consequence of the aging of insulating systems will eventually be a degradation of the material. Degradation can be described as an irreversible change in the material, where the electrical properties of the material also change. One may distinguish the terms *"aging"* and *"degradation"* by how they affect the breakdown voltage of the material. Aging can result in the degradation of the material. However, it may not directly reduce the breakdown voltage of the material. Degradation of the material, however, is a process that, in several cases, reduces the breakdown voltage [23]. When a dielectric is degraded, the result will eventually be a breakdown of the material. The breakdown of solid dielectrics, as XLPE, involves irreversible destruction of the material, resulting in failure [11]. The processes of electrical breakdown will be explained further in subsection 2.4.

The degradation of XLPE can be a result of electrical, chemical, and physical aging. While electrical aging depends on an electric field's application, chemical and physical aging happens without it [23]. An increase in local stress can initiate partial discharge (PD) activity, electrical trees, and water trees, which are the main processes causing the degradation of XLPE [23]. A PD occurs when a local discharge occurs in a weak region in the material, not bridging the full span between the electrodes. A full discharge implies an entirely conducting path through the dielectric. Thus an electrical breakdown of the material [15, 24].

2.2.1 Electrical aging

Applying an electrical field to XLPE for some duration will subsequently cause a reduction in the electrical strength of the material [11]. Specifically, XLPE encounters space charges (electrons, holes, ions) under a DC application. As a result of a constant applied voltage related to DC, the space charges accumulate in the material. Consequently, the electrical field will vary. Therefore, the stress experienced on an HVDC system will differ from an HVAC system [25]. The space charges can move in the material and become trapped in the bulk. Trapped charges could build up heterocharge, subsequently giving rise to local stresses and increasing the field locally at the electrodes [23]. Also, a strong enough field, with further assistance from temperature, can cause charge carriers to gain sufficient velocity between matrix collisions and trapping events and occasionally cause damage to the polymeric matrix. Both destruction of polymer XLPE chains due to chemical aging and a nonuniform electrical field impact trapped charges in XLPE [11].

2.2.2 Chemical aging

In the aspect of environmental factors, chemical aging is highly relevant. Chemical aging of XLPE involves different processes. One process is oxidation, which results from exposure to ambient conditions. Another element contributing to chemical aging are the by-products resulting from the crosslinking process [11]. Due to the necessary crosslinking agents used in the reactions, there will be different by-products left in the material after the crosslinking has taken place [26]. The by-products can be, for instance, acetophenone, cumyl alcohol, α-methylsyrene, methane, and moisture [11, 27]. Consequently, the by-products contribute to the generation of negative heterocharges. Under the application of DC voltage, such charges higher the electrical field locally at the electrodes in XLPE [28]. Other processes causing chemical aging are scission of polymer chains and depolymerization [23, 11].

Considering electrical measurements on XLPE insulation, the by-products can influence obtained results. Therefore, it is desired to perform a thermal treatment of the material previous to testing. The treatment aims to make the material stable, subsequently providing reproducible measurements. In addition, possible internal comparison of measurements gains higher reliability. According to an experimental study, it was suggested that in order to achieve an acceptable reduction of residue products in XLPE, the thermal treatment should be 48 h at 50°C [29]. In a report on the influence of thermal treatment and residues on space charge accumulation in XLPE, the results suggested that by-products in the material led to generation of heterocharge. Opposite, homocharge or no charge was seen when the XLPE had a pre-thermal treatment [30].

2.2.3 Physical aging

Physical aging of XLPE involves an internal change in the structure and morphology of the material. Temperature changes can induce motion in the polymer chains, which subsequently results in physical aging. Mechanical forces give rise to physical aging since such stress lead to an induction of microvoids and cracking in the material [24]. Considering how the physical aging of XLPE may affect the electric aging and degradation of the material, microvoids in the insulation could initiate PD activity and electrical treeing [11].

2.3 Charge injection and charge transport

Ideally, insulating materials would completely prevent the flow of electrical charges, thus never conduct. However, this is not possible as even insulating material with extraordinary electrical properties (in terms of insulation) will be conductive in some manner [15]. For the material to conduct, electrical charges must be present. With an applied electrical field, the electrically charged particles can be moved through the material. Therefore, the phenomenons charge injection and charge transport are relevant to consider. Charge injection and charge transport are dependent on how polymers behave as band-gap insulators. The band-gap model is based on the circumstances of different levels of energy in a material, where the electrons can go from the valence band to the conducting band, resulting in electrical conductivity. The energy gap between the levels results in a barrier between the levels, making it hard for the electrons to move to the conducting band. However, it should be noted that the situation in real life does not directly correspond with the ideal band gap model. The ideal band gap model of PE predict low charge injection, but due to traps in the material in real life, the opposite happens [24].

Considering charge injection, factors such as temperature and a high electrical field can lead to an injection of charge into an insulating material from electrodes. Consequently, the high field can also contribute to the electrical charges being transported through the bulk of the material. The charge injection is dependent on defects of the material. For instance, surface roughness and uneven contact (physical defects), contaminants and chemical residues as moisture (chemical defects), and trapped charges (electric defects) [24].

Two experimental studies suggest that the generation of charges, especially negative heterocharges, in XLPE under the application of DC voltage is highly dependent on inclusion in the material [28]. The inclusion happens as a result of by-products after crosslinking, including moisture, and by-products after oxidation [28, 31].

2.4 Electrical breakdown in solid dielectrics

In the aspect of DC breakdown in polymers and the deterministic process leading to breakdown, both charge injection and charge transport are important. Under the application of voltage and, thereby, an electric field, it is possible to reach a field where the situation within the dielectric becomes unstable. If the application of voltage is not reduced, such instability involves a rise of the current to a level that eventually can result in a discharge [24]. The initiation of full discharge in solid dielectrics, thus an electrical breakdown, occurs at the weakest point in the material [11]. Considering XLPE, if the polymer chain is damaged, there will be a point in the structure of the material being weaker.

In the categorization of electrical breakdown, the type of mechanisms present decides the type. Electrical breakdown may be categorized as one of the types listed under [23].

- Fast breakdown processes
- Degradation phenomenons
- Slow aging processes

Degradation phenomenons and slow aging processes are already reviewed in subsection 2.2. Several studies and different theories on the electrical breakdown of polymers can be found. Common for all of the studies is that aging subsequently could lead to sub-micro-cavities and more frequent regions of trapped charges. This is often the base for an eventual fast breakdown process [23].

Considering the fast breakdown processes, thermal, electric "intrinsic", and electromechanical breakdown are relevant. Fast breakdown processes can be classified as fully destructive, where the dielectric strength of the material is permanently lost. The breakdown mechanism dominating an eventual electrical breakdown varies and is a result of the applied electrical field, temperature, and stress history of the material [24]. Explanations of the fast breakdown processes are taken from the Specialization project [1], where necessary modifications have been done.

Mechanisms associated with electric breakdown are Zener breakdown and avalanche multiplication, where the latter is a process involving carrier impact ionization. An increase in the amount and density of charge carriers can subsequently result in multiplication of the charge carriers. Considering breakdown in polymers, the process of avalanche multiplication is contentious, but it may be possible for certain conditions. Through experimental testing, it is shown that "intrinsic" breakdown strength in some cases can be related to the Fowler-Nordheim process, where the breakdown is highly affected by the interface between the electrode and the polymer [24].

An electromechanical breakdown is related to cases where the breakdown is a consequence of the electrostatic attractions of electrodes. The attraction will affect the material such that the insulation experiences a loss of width. As the width is smaller than intended, the electrical field increases if the voltage is held at its preceding level. Such breakdown is impossible for XLPE (vs. PE) as it remains mechanically stable above the melting temperature [24].

The reason for thermal breakdown is simply explained as a situation where the heat generated is higher than the heat dissipated. Such a situation can occur locally, in a small spot, or in a larger part of the material. It is most common to occur in a small spot. The heat generated is a result of energy losses as a consequence of the current flowing in the insulation at applied voltage [15].

Directly given from the Specialization project [1]; different types of insulating materials have different electric properties. In the aspect of electrical breakdown, dielectric strength is a highly relevant parameter. This is because it governs how high electric field strength the material is able to withstand without a disruptive discharge occurring. Unlike in gases or liquids, in solids, a disruptive discharge will cause loss of dielectric strength, which is not possible to re-establish [23]. For solid dielectrics, such discharge cause a breakdown channel which can be seen as a hole through the insulation. The dielectric strength of a material is found by the maximum voltage possible to apply at a specific thickness of the material before breakdown occurs [15].

2.5 Prequalification Tests

In the aspect of ensuring a reliable power system, components must undergo testing previous to installation. A variety of tests based on different categories must be done to validate the functionality under operation. IEC and Cigre provide standards for recommended testing of components, including cable systems. Cigre gives recommendations for testing of DC extruded cable systems for power transmission at a rated voltage up to and including 800 kV in TB852 [32]. One category of testing is prequalification (PQ) tests. PQ tests are essential considering the long-term performance of power cables [8]. In TB852, the PQ tests involve a long-duration voltage test minimum of 360 days [32]. Under this test, the cables experience different cycles of stresses, which together represent the thermo-electrical stress expected throughout the lifetime of the cable [8].

For HV cable systems, the expected lifetime is over 30 years. The cables themselves are designed such that the economic lifetime is 40 years. However, the actual lifetime of a cable is predicted to be even longer [8].

2.6 Dielectric Breakdown testing

2.6.1 The stochastic behavior of electrical breakdown

The explanation of the stochastic behavior of electrical breakdown is from the Specialization project [1], where slight corrections have been made. In addition, theory on 95% confidence intervals is presented.

Examination of the breakdown strength of dielectrics is done by obtaining data on the breakdown voltage at a certain material thickness. Such data is obtained by applying voltage over the relevant test object using two electrodes [33]. Increasing the voltage between the electrodes will result in a breakdown. It is observed that doing several tests will not give the same breakdown value each time [15]. The reason for this is that electrical breakdown is a stochastic variable that varies with physical and chemical properties. Therefore, it is required to use statistical methods to estimate breakdown values [15, 34]. As the breakdown voltage is statistically distributed, it is helpful using distribution functions to perform a statistical analysis [15]. For reliability analysis, considering breakdown voltage and breakdown strength of dielectrics, the Weibull distribution is beneficial [35]. Weibull distribution is suitable for the extreme values of a distribution (minimum and maximum values). In Equation 2.1 the 3 parameter Weibull distribution is given [15].

$$P(E) = 1 - exp(-(\frac{E - E_{min}}{\alpha - E_{min}})^{\beta}) \tag{2.1}$$

In Equation 2.1, α is the scale parameter which is the electric field in kV/mm that gives 63.2% probability of breakdown. E_{min} is the lowest field that causes breakdown, and β is the shape parameter, which is a unitless parameter. The shape parameter establishes the base for the deviation in the distribution, as this parameter gives the slope of the function. It reflects the breadth of a distribution [15, 34]. In addition, the beta value indicates how the failure rate of the analyzed component behaves [36].

$\beta < 1$ indicates a failure rate that decreases as a function of time

$\beta = 1$ indicates a constant failure rate

$\beta > 1$ indicates a failure rate that increases as a function of time

Together, the three different regions of beta reflect the "bathtub curve" seen in Figure 2.2.

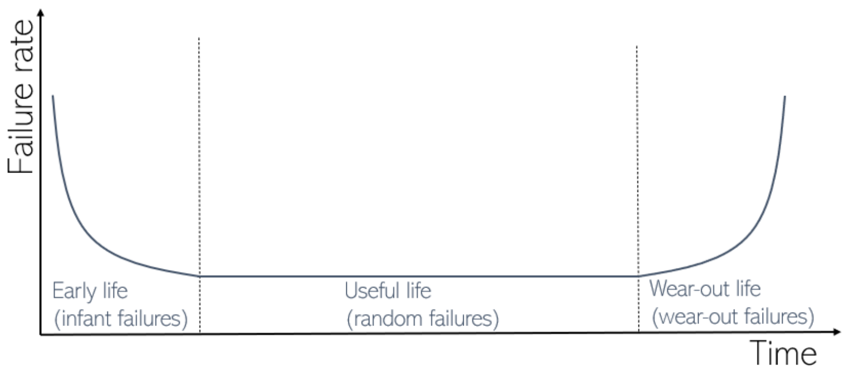

Figure 2.2: Bathtub curve. The illustration is inspired by Figure 1 in reference [37].

Decreasing failure rate is early failures, a constant failure rate indicates random failures, and an increasing failure rate gives the wear-out failures [37].

Considering the lowest possible breakdown voltage, there will be problems giving one correct value. It is also possible to make a good fitting for experimental data with different values of the parameters set together. This makes the use of 2 parameter Weibull distribution function typical in the matter of estimating the breakdown strength of solid insulation. The parameter E_{min} is set to zero, and the resulting function for such a distribution is given in Equation 2.2 [15].

$$P(E) = 1 - exp(-(\frac{E}{\alpha})^{\beta}) \tag{2.2}$$

In a statistical analysis, some uncertainty will always be related to the obtained results. The obtained results will depend on the collected data and the amount of data. Because of this, it is highly preferable to determine the confidence intervals (CI) or the confidence level of the data set. These two statistical parameters are related to each other, where the CI gives the interval for which the results are expected to end up. The confidence level is defined as a percentage, which gives the percentage of times the obtained values will lay within the specific confidence interval. In analysis, a 95% confidence level is highly used [38]. Regarding the Weibull distribution and dielectric breakdown, it is relevant to examine the confidence level for the scale and shape parameter [15].

2.6.2 Challenges with destructive tests on solid dielectrics

In terms of electrical breakdown of XLPE, such testing involves destructive tests on solid dielectrics. Each test is entirely destructive, and the dielectric strength is impossible to re-establish. Therefore, destructive tests on solid dielectrics require a large amount of test material. In addition, the test samples of the insulation should be as identic as possible. Therefore the test samples should be made using the same technology. However, the test samples will vary, and inequalities will be found in different batches of insulation. The material matrix varies due to variations in chemical structure and the amount of possible contaminants. In addition, the storage of polyethylene can change the material matrix and reduce its strength [33].

Considering the test samples, keeping the material smooth and clean is crucial as scratches can contribute to an uneven field distribution, consequently enhancing the local field [15]. Another factor that may affect breakdown values obtained from testing is the geometry of the used electrodes [33]. For instance, damaged/deformed electrodes give different results than undestroyed ones.

Since electrical breakdown is a stochastic phenomenon, there will be a difference between theoretical breakdown models and actual, practical breakdowns. Statistical analysis is necessary for reliability estimations, and expected breakdown values and values found in experiments are not directly comparable. For statistical analysis, a characteristic breakdown value is found for the given distribution, for instance, the 63.2% characteristic breakdown value in the Weibull distribution [24]. Furthermore, in experimental work, there could be an electronic "intrinsic" breakdown where the found breakdown strength will be higher than for practical cable insulation. [15].

Destructive tests on solid dielectrics often involve thin test samples of the desired material. The breakdown strength of thin films of insulation is seen to be higher than for thicker insulation.

From experience, the breakdown field decreases with increased sample thickness, known as volume effects [33]. The breakdown field also decreases with increased time for field application [24].

2.7 State of the art of DC breakdown testing on XLPE insulation

Research on how DC voltage application influences XLPE has increased throughout the years [9]. With this, experimental work has been performed aiming to collect data on how the electrical properties of XLPE may change under a DC field. In addition, studies with different focus areas are conducted where the experimental work has developed as measurement methods were improved.

Study 1

One study involving DC breakdown testing is from 2005, named *"Electric Characterization of Films Peeled from the Insulation of Extruded HVDC Cables"* [39]. The motivation for the work was related to the extrusion process of PE, more precisely, the cooling afterward. The hypothesis was that as PE is extruded onto a cable, the cooling will vary with time, depending on the radial position in the insulating layer. Since XLPE is a semi-crystalline material, a layer of such material will consist of different regions where the regions are dependent on factors present in the cooling process. With changing time-temperature schemes, the insulation's microstructure and the chemical composition of by-products will vary.

It was expected that the insulation in the region near the inner semiconductor would have improved crystalline structures relative to the insulation near the outer semiconductor. The explanation for this is that the regions near the inner semiconductor will have a slower cooling process and, thereby, a better progression of crystallizing. Further, the aim was to investigate whether the electrical properties would differ relative to the radial position in the insulation layer. One of the electrical properties investigated was the breakdown strength under the influence of DC field [39].

The method of obtaining data on the DC breakdown strength was to test cable peelings made from XLPE insulation. The condition of the insulation is not described. The cable peeling was cut from a $1200mm^2$ XLPE cable, where the peeling obtained a thickness of 100 µm. The peeling was cut continuously from the outer semiconductor to the inner semiconductor from cable parts of 55 mm. As it was aimed to investigate a possible difference in breakdown strength based on radial position, the tests were performed on insulation 0.5 mm from the inner semiconductor and 1 mm from the outer semiconductor. Before testing, the test samples were degassed for 24h under vacuum at 50°C.

The test cell consisted of a high voltage and ground electrode with diameters of 25 mm. In the test cell, Galden fluid was used. Galden fluid has good dielectric properties and is highly operational under low and high temperatures, making it fit different fields of use. For example, it is used as heat transfer fluid and for electronic testing. It can also be used as a solvent and in vapor phase soldering processing [40]. The tests were performed at 30°C, where the voltage was increased with a rate of 500 V/s until breakdown occurred. Thirty tests on each of the two different regions in the insulation were conducted. After testing, the data was analyzed using Weibull distribution [39].

The obtained results treated with the Weibull distribution function and the 95% confidence interval of the parameters, are shown in Table 2.2. All values are taken from the presented study [39].

Table 2.2: The obtained scale and shape parameter for the DC breakdown tests and the 95% confidence interval of the parameters.

Test region	α [kV/mm]	β
Near inner semiconductor	440 *95% confidence interval: 420-461*	9.8 *95% confidence interval: 6.6-12.6*
Near outer semiconductor	451 *95% confidence interval: 430-474*	9.8 *95% confidence interval: 6.6-12.8*

From the estimation, it is given that the 95% confidence interval for scale and shape values are overlapping. Therefore, the study concludes with no significant difference in the DC breakdown strength between the insulation near the inner and outer semiconductors. The further conclusion also implies that the differences in cooling under the extrusion process of the insulation do not influence the DC electric properties. The conclusion is based on both DC breakdown tests and measurements on the DC electrical resistivity [39].

Study 2

Another study on the DC breakdown strength of XLPE insulation was performed in recent years. The study is from 2017 and involves *"DC Electrical Breakdown Dependence on the Radial Position of Specimens Within HVDC XLPE Cable Insulation"* [35]. It aims to investigate if the radial location in the XLPE insulation layer of an HVDC cable will have a difference in the DC breakdown strength. The investigation also involves testing under different conditions of temperatures; 30°C, 50°C, 70°C, and 90°C.

The background for the desired investigation implies the theory regarding temperature gradients and varying cooling rates after the excursion process under the manufacturing of a cable with XLPE insulation. The hypothesis is that the different temperature gradients may lead to varying dielectric properties in the material. The study refers to experimental work where it is stated that considering the by-products after cross-linking, the amount of these is higher in the bulk of the insulation than in the area of insulation near the semiconductors. Several studies have been conducted on how this may affect the AC breakdown strength in different insulation regions, but no standard answer has been found

The experimental work involved DC breakdown tests performed on three different regions of the XLPE insulation; insulation near the inner semiconductor, middle insulation, and insulation near the outer semiconductor. Furthermore, information on the insulation's physical, chemical, and thermal condition was obtained. Used methods for obtaining such information were Fourier Transform Infrared spectroscopy (FTIR), differential scanning calorimetry (DCS), scanning electron microscopy (SEM), and X-ray diffraction (XRD).

Similarly to Study 1, this study utilized XLPE insulation specimens in the form of cable peeling. The cable peeling was cut continuously from the outer semiconductor to the inner semiconductor from a ±160 kV HVDC XLPE cable. The HVDC cable was an unaged cable with an insulating layer of 16 mm. For the manufacturing of the cable peeling, a microtome was used. When performing the DC breakdown tests, the test samples were in the form of discs of 60 mm.

The setup for the DC breakdown tests consisted of an HV electrode and a ground electrode made of stainless steel. Both electrodes had a diameter of 25 mm and were rounded to reduce the electrical field at the edges. The electrodes were arranged in a test cell with vegetable oil. For each measurement, a test sample was sandwiched between the electrodes, and the DC voltage was increased manually with 1000 V/s. A total of 16 tests were carried out for each of the three insulation regions. The thickness was measured with a thickness meter to determine breakdown strength in kV/mm. Three thickness measurements near the breakdown channel were conducted. After that, the average was found. The resulting thickness was 200 µm ±20 µm. Tests leading to breakdown at the electrode edges were not included.

The obtained data on DC breakdown strength was analyzed using 2-parameter Weibull distribution. The study provides four Weibull plots for the DC breakdown of XLPE for each of the four different temperatures, where the plots contain the 95% confidence interval for the tests performed on each region. Additionally, all the scale and shape parameters were given in a table. The results of DC breakdown measurements performed at 30°C are given in Table 2.3. All values are taken from the presented study [35].

Table 2.3: The obtained scale and shape parameter for the DC breakdown tests performed at 30°C.

Test region	α [kV/mm]	β
Near inner semiconductor	437.6	19.30
Middle insulation	405.4	10.79
Near outer semiconductor	429.3	15.68

The results from the breakdown testing showed that the DC breakdown strength obtained at 30°C, 50°C, and 70°C is lowest for the middle insulation relative to the two other regions. The results from the other methods gave the following:

- Results from FTIR show a higher amount of by-products in the middle region of the insulation.
- DCS had results showing a little higher crystallinity of the middle insulation.
- SEM indicates a difference in the physical features of the regions, where the middle regions of XLPE have varying grain sizes. In addition, higher irregularity in the molecular chain in the middle region is observed.
- The XRD analysis supports the results from the three tests listed above.

The conclusion regarding the tests performed at 30°C, 50°C, and 70°C is that together, the higher amount of by-products, the varying grain size, and higher interplanar spacing in the crystalline structure result in lowering the DC breakdown strength of XLPE. Evaluating the results from the tests performed at 90°C, the DC breakdown strength in different insulation regions is not significantly varying. Less variation can be due to the findings in the DCS and SEM analysis, showing less regularity in the molecular structure in the middle insulation at 83°C. Furthermore, the study concludes that the DC breakdown strength is exponentially reduced with increasing temperature.

3 Experimental work

The experimental work of this Master's thesis involved breakdown testing of XLPE cable peeling under the influence of a DC field. To investigate how the condition of the insulation changes as the insulation ages, DC breakdown tests were performed on both fresh and aged cable peeling. The insulation layer of an HVDC cable is thick. Therefore, obtaining statistics on different parts of the insulation was also desired to examine if the radial position in the insulation affects breakdown strength.

In the preliminary work, a test setup was established, and breakdown testing of XLPE cable peelings under the influence of an AC field was performed. From the experimental work in the preliminary study, it was concluded that the setup gave reliable results that corresponded with earlier studies on AC breakdown. Therefore, it was plausible that the setup, especially the test cell, would also be functional for DC breakdown testing.

This section describes the methodology followed to obtain data on the DC breakdown strength of XLPE cable peeling. The information given in the section is listed below.

- An explanation of the test setup and the functionality of the different parts of the circuit.
- A more detailed description of the chosen electrodes and the established test cell.
- Information on the test object(s).
- The applied DC signal.
- The circumstances for the DC breakdown testing.
- Detailed description of the methodology.

3.1 The Test setup

In the lab, the test setup comprised components from the preliminary work and newly incorporated elements. To obtain data on the DC breakdown voltage of the solid dielectric, it was necessary with a circuit generating a stable DC voltage and the possibility to measure the breakdown voltage securely. Figure 3.1 shows a schematic presentation of the circuit.

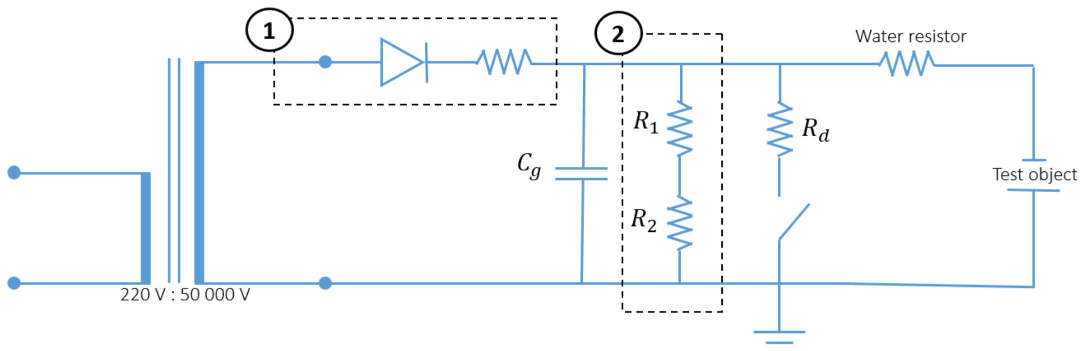

Figure 3.1: Electric circuit used for DC breakdown testing. *1:Half-wave rectifier. 2:Voltage divider for voltage measurement.*

A transformer in series with a half-wave rectifier was used to generate DC voltage. The half-wave rectifier is marked as 1 in the figure. To minimize the AC ripple and obtain a stable DC voltage, a smoothing capacitor, C_g was coupled in parallel. The next branch, marked as 2, is a voltage divider with the purpose of enabling measurement of the DC breakdown voltage. An earth breaker, a water resistor, and a test cell are seen in the last part of the circuit. The earth breaker provided the ability to discharge the circuit after each test, while the water resistance reduced the short circuit current upon a breakdown.

The HV transformer was a Ferranti coupled to the relation of 220 V on the primary side and 50 kV on the secondary side. It gave a voltage application of the frequency of 50 Hz. For the half-wave rectifier, the rated values were 140 kV, 20 mA, and 100 kΩ. The smoothing capacitor had a size of 25 nF. In the voltage divider, R_1 and R_2 had the values 280 $M\Omega$ and 28 $k\Omega$, respectively. Considering the obtained DC breakdown values, the voltage was measured over R_2 with a multimeter. The actual voltage over the test object was found by multiplying the measured voltage over R_2 with the relation between the resistances in the voltage divider. The relation is calculated in Equation 3.1.

$$\frac{R_1}{R_2} = \frac{280\ M\Omega}{28\ k\Omega} = 10\ 000 \tag{3.1}$$

For the discharge of the circuit, the earth breaker was coupled in series with a resistor, R_d. The size of the resistor was 2.4 kΩ. The water resistor, reducing the short circuit current, was measured to be 230 kΩ. In the schematic presentation of the circuit, the test object is seen to the right. In the actual circuit in the lab, the test object was placed within a test cell. The test cell and the test object are further explained later.

The elements of the circuit explained above are all a part of the HV side of the transformer. In addition to the test setup established on the HV side, there was a setup on the low voltage (LV) side as well. The setup on the LV side provided automatic adjustment of the voltage application. Figure 3.2 shows the setup of the different components regarding the automatic voltage adjustment and how the components were coupled. The arrows indicate the directions of the signals.

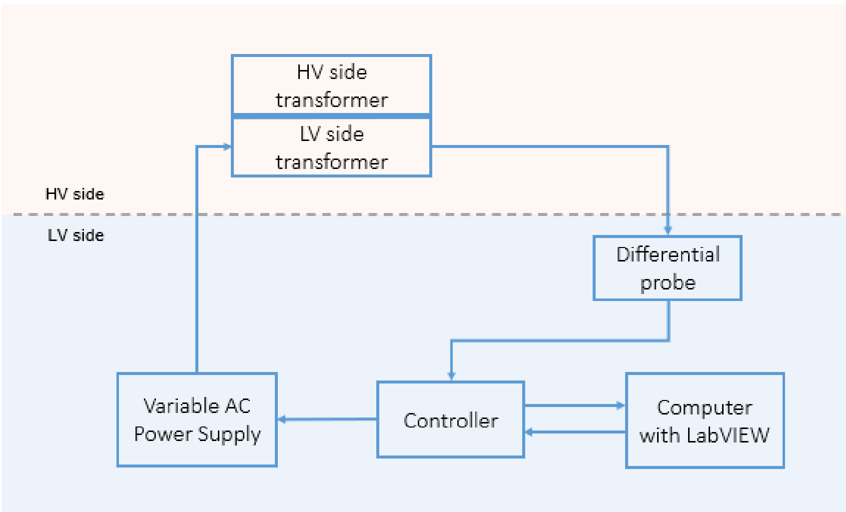

Figure 3.2: Setup for automatic adjustment of applied voltage.

In the figure, only the transformer from the HV side is presented. On the LV side, the setup consisted of a Variable AC Power Supply (variac), a controller, a differential probe and a computer with LabVIEW. The code in LabVIEW was set based on the given requirements for this project. The differential probe, giving voltage measurements to the controller, measured the voltage directly on the LV side of the transformer. Therefore, the automatic adjustment of the voltage was based on the transformer's primary AC voltage. Based on the settings in LabVIEW and the voltage measurements from the probe, the controller adjusted the voltage on the exit of the variac. The exit of the variac set the voltage on the primary side of the transformer. In the LabVIEW program, the following parameters were set:

- Start Voltage [kV]
- Stop Voltage [kV]
- ΔV [kV]
- Δt [min]

These parameters describes the AC voltage at the secondary side of the transformer. The description of each parameter to be set in LabVIEW is taken from the Specialization project, involving necessary correction.

When the code for the automatic adjustment of the voltage was started, the voltage would increase from 0 V to the given start voltage. If the value for the stop voltage were reached, the code would stop. The voltage was increased with ΔV for each Δt, where Δt was the time interval for how long the voltage was held at one voltage value. The set values are presented in a later subsection. The variac operated in a way where it coupled out contactor two (K2) at a breakdown, making the output voltage from the transformer zero. When the probe for the controller measured zero voltage, the LabVIEW program stopped. The program's functioning is not explained further, as NTNU's electrical workshop provided the code used in LabVIEW [1].

3.1.1 Electrodes

The section on the electrodes is highly inspired by the description of the electrodes given in the Specialization project [1]. Necessary modifications have been made to better understand the geometry.

When designing the electrodes for the test cell, there was an aim to consider what impact the geometry of the electrodes would have in the context of testing. The electrodes can be seen in Figure 3.3a, as well as an illustration with the dimensions can be found in Figure 3.3b.

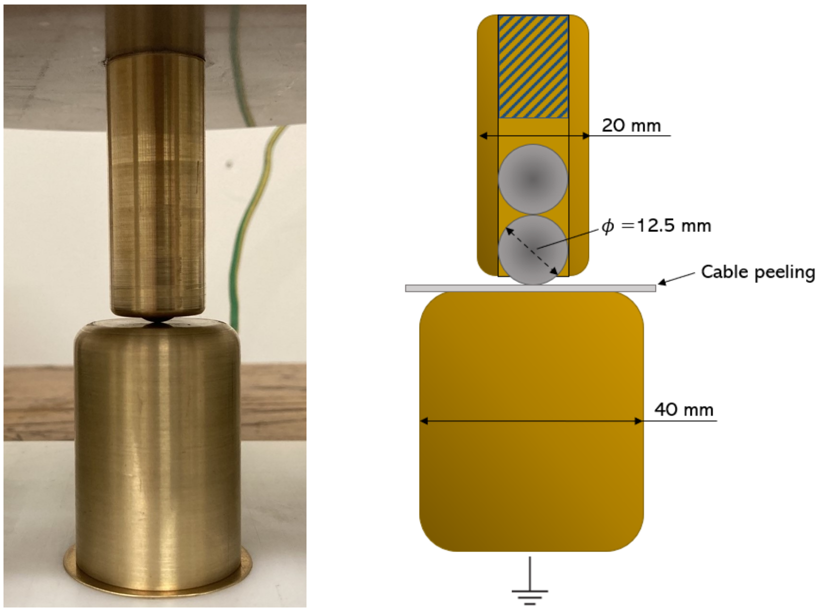

(a) Physical setup of the electrodes.

(b) Geometry of the electrodes.

Figure 3.3: High voltage- and ground electrode.

Both the HV electrode and the ground electrode were made of brass. The design was a sphere-plane geometry, where the HV- and ground electrode were 20 mm and 40 mm, respectively. The ground electrode was chosen to be wider than the HV electrode to avoid air bubbles in the oil around the tip of the electrodes. In addition, the electrodes were rounded to prevent large electric fields at the edges of the electrodes.

As well as rounding of the tips, the HV electrode had a bearing ball. The bearing ball was made of steel and had a diameter of 12.5 mm. The bearing ball prevented pitting contact. A hole was made in the HV electrode for the bearing ball, making it possible to change it regularly. The distance between the electrodes was 1 mm, excluding the bearing ball. In the HV electrode, a thread was assembled, which connected the rest of the circuit. In Figure 3.3b, the blue imprint in the HV electrode is the area where the threaded fastener was implemented. In the hole in the HV electrode, an additional bearing ball was placed over the bearing ball touching the sample. This arrangement made a light pressure on the test object under testing.

3.1.2 The Test cell

The test cell was established and constructed in the Specialization project, and no further changes were carried out. The information on the test cell is taken from the Specialization project [1], with a few modifications.

The test cell was designed to apply both HVAC and HVDC voltage to the cable peeling. It consisted of a container filled with oil, an arrangement for holding the HV- and ground electrode, and an arrangement for fastening the test object. The setup in the container was chosen with the aim of making the position change of the test object as undemanding as possible.
Figure 3.4 gives a closer view of the test cell.

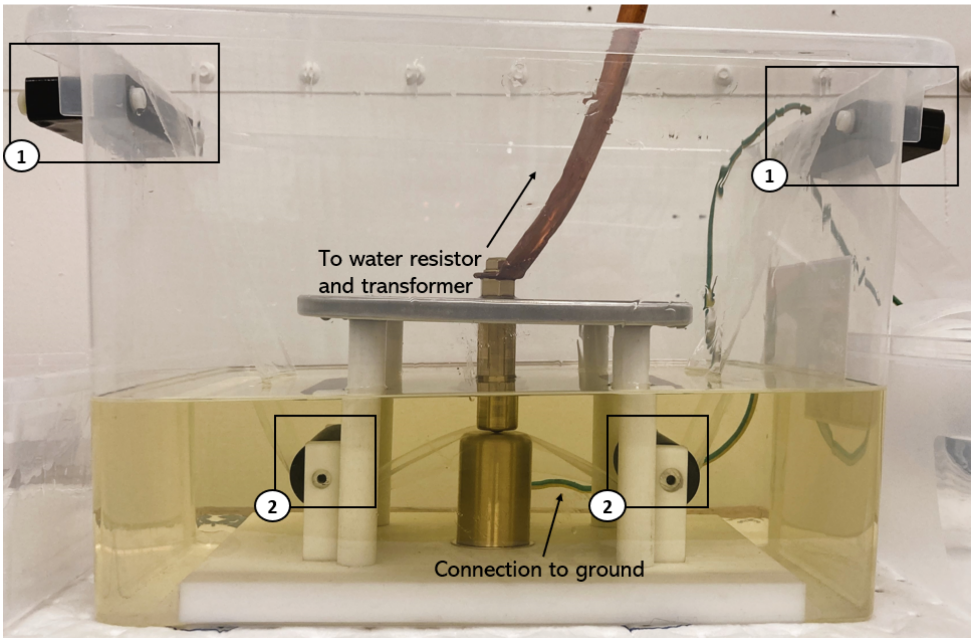

Figure 3.4: The test cell. *1:Fastening points for the test object. 2:Drums to enable easy position change of the test object.*

The electrodes were placed in the middle of the arrangement in the test cell. The arrangement consisted of an insulating plate in the bottom and insulating supports made of Polyoxymethylene (POM), also known as acetal. POM is a type of plastic often used for different components in the engineering industry due to its good material properties. For instance, it has high fatigue strength, is resistant to wear, and has low friction making it functional in constructions involving sliding [41]. The supports kept the metal plate up. Together, this arrangement set the base for the HV- and the ground electrode. On both sides of the electrodes, two cylindrical drums made of POM can be seen. When establishing the design of the test cell, the bolts, which fastened the drums, were changed from steel bolts to Lexan bolts. The purpose of this was to avoid floating voltage potential. The arrangement with drums made it possible to pull the cable peeling through the arrangement. At the top of the test cell's outer surface were two fastening points. These provided the ability to apply tension to the peeling. With tension, the peeling between the electrodes was stretched out, ensuring the peeling lay flat between the electrodes. The oil filled in the cell to prevent external flashover was MIDEL 7131. This is a synthetic ester transformer fluid.

In addition to the container composing the test cell, two more containers were placed on each side of the test cell. One of the containers was the "start station" for the test object, which was aimed to be as clean as possible. Therefore the container was wiped off with isopropanol frequently. The other container was the "end station" for the test object after being soaked in oil.

3.2 The Test object

To collect data on the DC breakdown strength of XLPE cable insulation, the test objects were made of such insulation taken from an HVDC cable. As breakdown testing on solid dielectric implies irreversible destruction, a high amount of test specimens being as identical as possible is required. To obtain specimens satisfying such criterion, the test objects were in the form of cable peeling. Figure 3.5 shows an example of an unused test sample of cable peeling.

Figure 3.5: A test sample of cable peeling.

The cable peeling was cut from a full-scale cable end of a 525 kV HVDC cable, where the test samples were obtained from fresh and aged cable insulation. For this study, all the test samples were cut from the same cable with the same production run:

1. The cable was made in a cable tower and subsequently degassed to remove by-products from the cosslinking of PE.
2. QC (quality control) was performed, which involved AC screening and checking the used PE pellets, for instance, in the aspect of contaminants.
3. The cable got an outer covering and was assembled on a drum.
4. Two different specimens from the same cable were made; from these the cable peelings were cut.

One of the specimens was collected from the drum and taken through PQ tests following standards like Cigre TB 496: *"Recommendations for testing DC Extruded Cable Systems for Power Transmission at a Rated Voltage up to 500 kV"* and Cigre TB 852: *"Recommendations for testing DC extruded cable systems for power transmission at a rated voltage up to and including 800 kV"*. After the PQ test, a super-imposed lightning and switching test was performed, and finally, a DC withstand test. This specimen gave the aged cable peeling. The other specimen was collected from the drum referred to in point number three. Thereby this cable peeling is the fresh (unaged) cable peeling, which will be considered as the reference point regarding the condition of the insulation. Until the cable peeling was manufactured from the specimen with fresh insulation, the cable was stored on the drum with an impermeable metallic water barrier. Thus, this insulation did not age.

A knife and a lathe were used to manufacture the cable peelings. The insulation was manually cut from the outer semiconductor to the inner semiconductor. Due to the manual cutting, the thickness of the peeling samples could vary to some extent, but the aim was to achieve a thickness of 100 µm. Based on measurements, the variation was -2 µm to +15 µm. The width of the cable peeling was 70 mm.
On the cable peeling samples from the fresh specimen of insulation, a slot was drilled on the edge. This made it possible to keep track of the orientation in the insulation layer, as there would be a slot in each turn. Figure 3.6a shows an example of a marking of a turn.

Unfortunately, the slot was not made on the peeling samples from the aged specimen. Therefore the orientation in the cable peeling will be referred to as "inner XLPE", "middle XLPE" and "outer XLPE". The classification can be seen in Figure 3.6b.

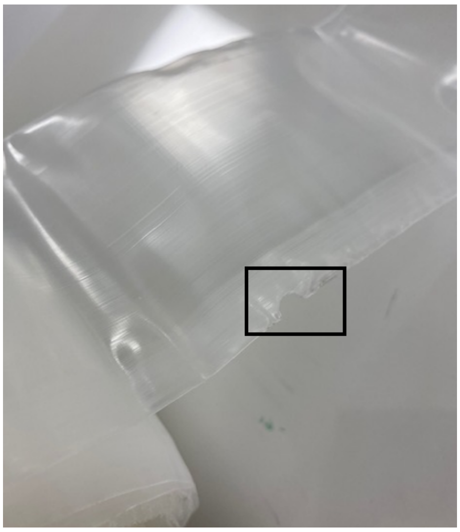

(a) A marking of a turn in the cable peeling.

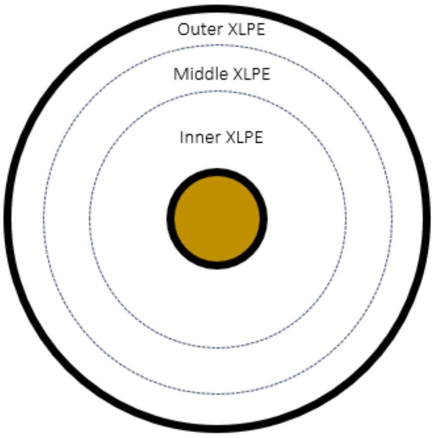

(b) Classification of orientation in the cable peeling samples. The classification is inspired by the work in reference [39].

Figure 3.6: Orientation within the cable peeling.

3.2.1 Preparation before testing

The test objects were sent from the manufacturer in separate plastic bags in a cardboard box. The box was filled with a desiccant to ensure maintaining low humidity during transport. After arrival, the cable peelings were cleaned with isopropanol to minimize the amount of possible dust particles after manufacturing the cable peeling, and to ensure clean samples without grease marks. After cleaning, before testing, the cable was set in a heating cabinet to be degassed and to remove possible humidity. The thermal treatment was done for 24 hours at a temperature of 40°C. The temperature was set to 50°C for the last hour of degassing.

3.3 Collecting data of DC breakdown strength

The experimental work in the lab consisted of several parts. The first part was preliminary testing, where the aim was to make the automatic voltage adjustment as precise as possible. The main testing included testing on cable peeling from the aged and fresh specimens of XLPE insulation. For each sample of cable peeling, three test series of 20 tests were done. The three test series were based on the area of the insulation. One series was performed on the insulation near the outer semiconductor, one on the middle insulation, and one on the insulation near the inner semiconductor. Further in the report, this will follow the classification "inner XLPE", "middle XLPE" and "outer XLPE" in Figure 3.6b.

3.3.1 The applied DC voltage

Considering the applied DC voltage and the automatic adjustment, two factors made it challenging. These two factors were the functionality of the variac and disturbances in the AC signal from the power distribution. Throughout the preliminary testing, the management of the automatic voltage adjustment was worked out and modified. The modifications ensured that the DC voltage signal was as correct and stable as possible.

Due to the functionality of the variac, there were certain limitations in the voltage control. When the desired voltage was to be set on the variac, it raised problems because the motor controlling the variac had trouble reaching the exact set voltage. Another factor directly influencing the DC signal was the disturbances in the AC signal from the available power distribution in the lab. Using an oscilloscope, measuring the AC voltage on the exit of the variac, different degrees of disturbances were seen. Furthermore, measurements done directly on the electrical outlet to which the transformer was coupled, showed signal variation. This signal was the one that was measured by the differential probe and which the controller operated after. Despite the disturbances in the AC signal, the DC signal can be seen to be a stable signal in Figure 3.7. It can also be seen that the AC ripple is minimized.

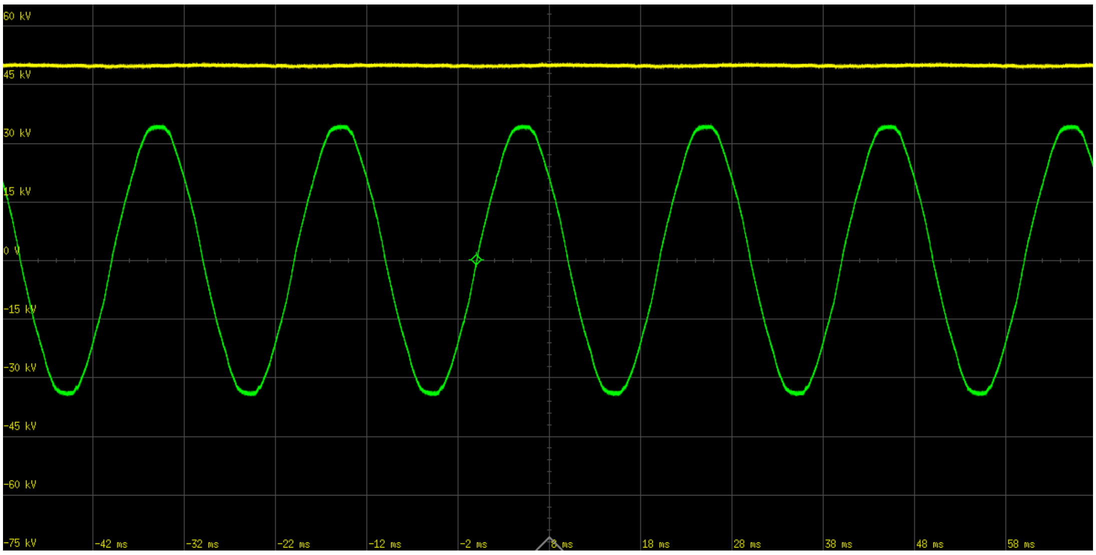

Figure 3.7: The AC signal on the primary side of the transformer, in green, and the corresponding applied DC signal in yellow. - *Screenshoot from the Digital oscilloscope.*

The variac's limitation and the AC signal disturbance caused problems regarding the automatic voltage adjustment. The code would adjust the voltage and always try to reach the "correct" step. Unfortunately, this would be impossible due to the disturbances and the issues with setting the output of the variac completely accurate. The tolerance in LabVIEW, associated with the step voltage, was increased to minimize the influence. The tolerance was set to 600 V.

3.3.2 Circumstances of measurements

Regarding the automatic adjustment of the voltage, it is two links between the measured voltage, which is the basis for the adjustment, and the actual applied DC voltage.

Link 1: The controller adjusted the voltage based on the measured value on the primary side of the transformer and the desired value on the secondary side (set in LabVIEW). LabVIEW calculated the voltage of the secondary side based on the relationship of the transformer, thus 220 $V/50\ kV$.

Link 2: Furthermore, the signal on the secondary side of the transformer was rectified to the DC signal that was applied over the test object. The automatic adjustment of the DC voltage over the test object would experience some inaccuracy because of multiple links preceding the actual applied voltage.

Other factors affecting the automatic voltage adjustment concern the inserted tolerance in the LabVIEW code. With a tolerance of 600 V, the sensitivity of the code, and thereby the adjustment from the controller, was reduced. As the sensitivity was reduced, the controller could increase the voltage on the variac with 1-2 adjustments. Thus the inserted tolerance was necessary to avoid the voltage being adjusted several times within a step. However, with the tolerance, there would be a slight margin of error when increasing the chosen voltage step, ΔV. The voltage would not increase at the exact voltage step but reach the step within a certain interval.

The disturbances in the AC signal not only impacted the automatic voltage adjustment but also influenced the registered DC breakdown voltage values. The DC voltage applied over the test object was measured using a multimeter which measured the voltage over R_2 in the voltage divider.

On the multimeter, a function was used where the highest voltage measured was saved on the screen. Because of the varying AC signal, the DC signal varied to some degree. Therefore, the obtained DC breakdown voltage would not be precisely correct. On the multimeter, the voltage was measured in the range of volts and showed three decimals. Due to the disturbances, the third decimal was not taken into account. The second decimal would also vary a little, so the margin of error on the registered DC breakdown voltage could be some 100 V when converting the measured voltage to the actual voltage in the kV range. Nevertheless, 100 V is not considered a significant variation in the kV range.

Before performing the main testing, the bearing balls in the electrode were changed. In addition, the ground electrode was polished. These measures were taken to ensure smooth surfaces without pitting. Throughout the testing on both aged and fresh cable peeling, the bearing balls were changed regularly, and the ground electrode was polished when needed. In addition, every time before assembling the test setup again, the bearing ball and the ground electrode were cleaned with isopropanol.

For storage of the cable peeling, a box with solid closing mechanisms was used, and each peeling sample was stored in double plastic bags. This was to prevent the cable peeling from being too heavily exposed to air and humidity. The humidity in the box was controlled during the periods of testing. The highest value of humidity was measured to be approximately 25 %RH, but typically the value was between 16-17 %RH.

3.3.3 Procedure for measurements

To obtain usable and comparable data on the DC breakdown strength of XLPE insulation, it was aimed to follow the same procedure for all measurements. The procedure can be divided into three main parts.

1. Set the parameters in LabVIEW
2. Perform DC breakdown tests
3. Thickness measurements of all the breakdown channels

The settings in LabVIEW, for the automatic adjustment of voltage had to be set relative to the secondary side of the transformer. As the breakdown of XLPE under the influence of DC voltage was the desired parameter to study, the step voltage was to be set considering the output DC signal. Therefore the relationship between AC voltage and DC voltage was needed. The relationship between the root mean square (RMS) value of AC voltage and DC voltage is given in Equation 3.2.

$$V_{DC} = \sqrt{2} \cdot V_{AC,rms} = 1,4142 \cdot V_{AC,rms} \tag{3.2}$$

The desired step of the DC voltage applied to the test object was 1 kV. The corresponding AC voltage in RMS value is calculated in Equation 3.3, using the inverse of Equation 3.2.

$$\frac{1\ kV_{DC}}{\sqrt{2}} = 0.7071\ kV_{AC,rms} \tag{3.3}$$

Each voltage step was decided to be held for 1 minute before the voltage would increase again. Considering the Stop Voltage, this was set to the maximum voltage value of the secondary side of the transformer, which was 50 kV AC. Due to some internal functionality in the LabVIEW code, the start voltage had to be 3 kV AC, for the code to be possible to start. All the chosen settings are summarized in Table 3.1.

Start Voltage = 3 kV AC
Stop Voltage = 50 kV AC
ΔV = 0.7 kV AC
Δt = 1 min

Table 3.1: Settings in LabVIEW. - *Relative to the secondary side of the transformer.*

A basic illustration of the corresponding DC step voltage applied to the test object throughout a test can be seen in Figure 3.8. However, due to the varying circumstances around the automatic voltage adjustment, the settings in LabVIEW were not precisely followed. Thus the illustration does not give the exact voltage adjustment progress.

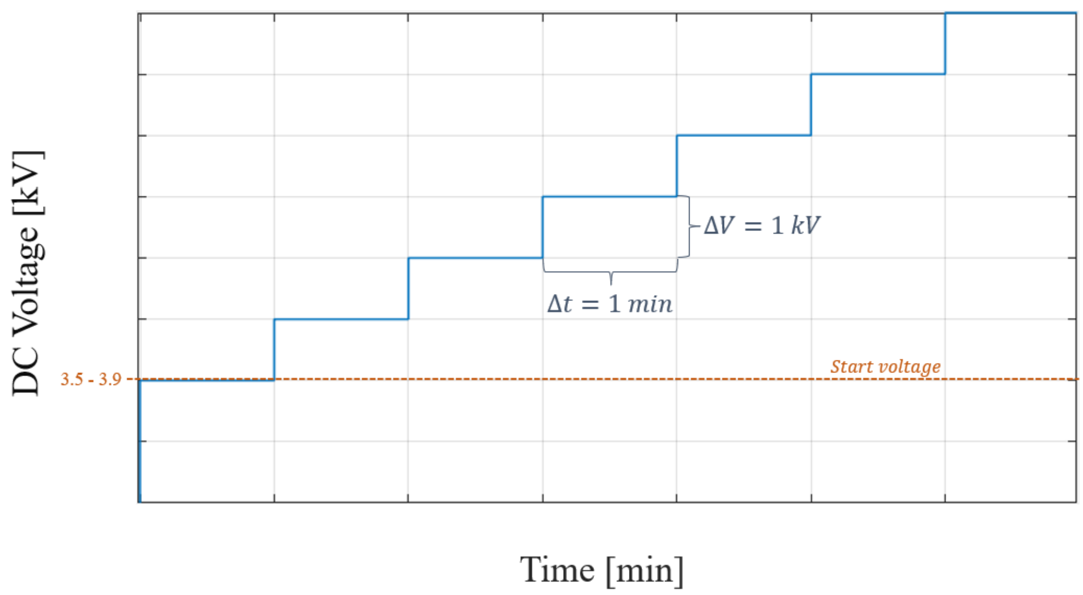

Figure 3.8: Basic illustration of the DC step voltage applied to the test object until breakdown.

In Figure 3.8, it can be seen that the start voltage would typically lay between 3.5 and 3.9 kV DC. This is based on observed values throughout all tests. The worst-case scenario for the adjustment would be that one step would be either 400 V or 1.6 kV. Based on observations from the first breakdown tests performed, the worst-case scenario happened two times. A majority of the steps were in the range of 800 V to 1.2 kV.

Before starting with the breakdown tests, the desired insulation area to test was decided. For the peeling sample from the fresh specimen, the orientation in the insulation was kept track of by counting the turns as the cable peeling was moved through the test cell. Due to no markings in the aged cable peeling, it was only possible to keep a rough track of the orientation within the insulation.

The DC breakdown testing can be divided into 6 series, excluding the tests performed in the preliminary work. The first three series are related to the aged specimen of insulation, and the three latter appertain the fresh specimen. The series can be seen in Table 3.2, where they, in addition, are numbered.

Table 3.2: The series of the DC breakdown testing. Based on the type of insulation specimen and region in the insulation layer.

Series	**Location in insulation**
1.1	Aged insulation - Outer XLPE
1.2	Aged insulation - Middle XLPE
1.3	Aged insulation - Inner XLPE
2.1	Fresh insulation - Outer XLPE
2.2	Fresh insulation - Middle XLPE
2.3	Fresh insulation - Inner XLPE

For all the series, the same steps were followed. First, the cable peeling was pulled through the test cell until the desired area for the specific test series was found. Next, the fastening points were tightened so that the part of the peeling sandwiched between the electrodes lay flat. Next, the voltage was increased until breakdown occurred, and the measured DC breakdown value was registered. The cable peeling was moved (approximately) to a new turn, depending on whether the particular cable peeling sample had slots for each turn. The fastening points were tightened again, and a new test was run.

Throughout the testing, a marking was cut in the edge of the cable peeling, where the breakdown channel could be found. After all 60 test on one cable peeling was performed, the thickness measurements of the breakdown channels were done. The purpose of this was to ensure a correct determination of the electrical field required to result in a breakdown. The thickness was measured after the breakdown tests to prevent damaging the peeling and possibly affecting the resulting breakdown voltage. Before the thickness measurements, the cable peeling was taken out of the test cell, and the oil was roughly wiped off. The used micrometer can be seen in Figure 3.9.

Figure 3.9: Micrometer used for thickness measurements.

The micrometer gave measurements with four decimals. Only three decimals were considered when determining the electrical field strength. The values were rounded off, but the fourth decimal was experienced to vary, meaning there will be some margin of error related to the obtained values. For some of the breakdown channels, three additional measurements were done to assess the thickness variation in a turn. In addition, it was used a digital microscope to inspect some of the breakdown channels. The used microscope was a Keyence VHX-600 with a Keyence VH-Z100R lens. The zoom range was of $100 - 1000$ times magnification.

All data obtained throughout the experimental work was logged in Excel, and can be found in Appendix B and Appendix C. Subsequently, the data was exported to MATLAB and treated there.

4 Results and Discussion

In this section, the results from the experimental work are presented, interpreted, and discussed. First, the DC breakdown strength determined based on DC breakdown testing and thickness measurement is given in two subsections:

4.1 The DC breakdown strength of aged XLPE cable peeling

4.2 The DC breakdown strength of fresh XLPE cable peeling

All the obtained breakdown strength values are plotted in a Weibull probability plot in MATLAB. In addition, the scale and shape values for the distributions are estimated with built-in functions in MATLAB. However, the method used in MATLAB to estimate the Weibull parameters is based on Maximum Likelihood Estimator (MLE). Therefore, the 63.2% characteristic breakdown strength given in the tables will not correspond directly with the Weibull probability plot.

An internal evaluation for both types of specimens is conducted, and the determined DC breakdown strengths are compared with the results from previous studies.

After the individual discussion on the results of each of the insulation specimens, a comparison is performed to evaluate if a distinct difference in DC breakdown strength can be found. The comparison is made in subsection 4.3.

After that, the focus is on possible errors in the measurements and weaknesses and strengths of the experimental work, found in subsection 4.4.

Since the breakdown tests are performed on insulation scaled down relative to actual cable insulation, the results from the experimental work do not directly correspond with values found for practical cable systems. Comments on this is found in subsection 4.5.

All presented values are DC voltage values if nothing else is stated. In the presented Weibull plots, any values from failed DC breakdown tests are excluded from the data sets. The DC breakdown voltage values obtained in the preliminary work will not be presented since this work only had the purpose of making the automatic adjustment of the voltage work.

4.1 The DC breakdown strength of aged XLPE cable peeling

In Figure 4.1, the obtained data on the DC breakdown strength of aged cable peeling is gathered in a Weibull probability plot. In addition, the resulting scale parameters ($\hat{\alpha}$), or 63.2% characteristic breakdown strength, and the shape parameters ($\hat{\beta}$) for the distribution of the three regions are presented in Table 4.1. Each color and type of marking indicate one region of the insulation.

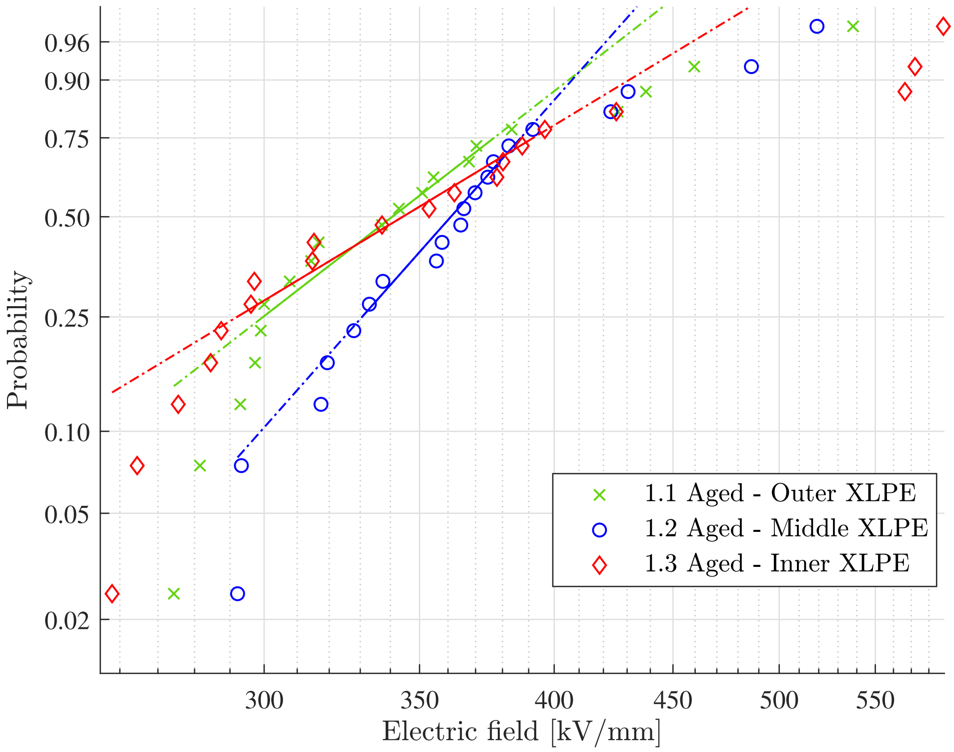

Figure 4.1: Weibull probability plot of the DC breakdown strength of the aged XLPE insulation. Each color and type of marking indicate one region of the insulation.

Table 4.1: Scale and shape parameter of the Weibull distribution for the three test series performed on aged XLPE insulation. The 95% CIs for the values are given in cursive.

Test series/region	$\hat{\alpha}$ [kV/mm]	$\hat{\beta}$
1.1 Aged - Outer XLPE	381 *95% CI: 348-418*	5.1 *95% CI: 3.7-6.9*
1.2 Aged - Middle XLPE	396 *95% CI: 368-427*	6.2 *95% CI: 4.6-8.5*
1.3 Aged - Inner XLPE	405 *95% CI: 358-459*	3.7 *95% CI: 2.7-5.1*

In Table 4.1, it can be seen that the region with the highest scale parameter is inner XLPE, with a 63.2% probability for a breakdown of the cable peeling at an electrical field strength of 405 kV/mm. Middle XLPE and outer XLPE have a scale parameter equal to 396 kV/mm and 381 kV/mm, respectively. The biggest difference in the scale parameter is an electrical field strength of 24 kV/mm between the inner and outer XLPE. The estimated 95% CIs for the scale parameters of the three test series are given in cursive in Table 4.1. It can be seen that the whole interval for the middle XLPE lies in between the interval for the inner XLPE. Considering the interval for the region of the outer XLPE, this overlaps partly with both the interval for the inner and middle XLPE. The overlap of the 95% CIs indicates that no significant statistical difference is found in the scale parameter of the three regions in the insulation. When analyzing the CIs, other aspects should be considered as well. For instance, the data size can influence the estimated CIs. However, to ensure higher reliability in the comparison, the data sets all have the same size, as 20 DC breakdown tests were performed for each region. The CIs also give information on the diversity of the obtained values, which says something about the uncertainty of the data set. For the three test series, the size of the intervals varies:

- Outer XLPE: (418 - 348) kV/mm = 70 kV/mm
- Middle XLPE: (427 - 368) kV/mm = 59 kV/mm
- Inner XLPE: (459 - 358) kV/mm = 101 kV/mm

It can be seen that the 95% CI for the region of inner XLPE has the most considerable interval. In contrast, the smallest interval is given for the middle XLPE. The smaller 95% CI suggests that the data set collected for the DC breakdown strength of the middle XLPE fits the distribution better than the data set collected for the inner XLPE. The length of the CI for the DC breakdown strength of the outer XLPE is closer in size to the interval of the middle XLPE than for the inner XLPE, where the difference is ≈10 kV/mm and 30 kV/mm, respectively. The lower CIs indicates that the values obtained on the DC breakdown strength of the outer and middle regions of XLPE better fit the 2-parameter Weibull distribution than the data of the inner XLPE.

Although the 95% CI indicates no significant difference in the DC breakdown strength of the three insulation regions, a slight difference is seen in the scale parameter. The difference can, first and foremost, be because an electrical breakdown is a stochastic variable. It is highly plausible that this is the main reason. Throughout the procedure of measurements, it was attempted to keep the stages as similar as possible for all three regions. One difference in the procedure that could affect the DC breakdown strength is the exposure of the test objects to ambient conditions. The test object was kept in the test cell from the start of testing on the outer XLPE until the final test series was performed on the inner XLPE. As the insulation was exposed to air for a longer time when the tests on the inner XLPE were performed, one may expect that the scale parameter should be the lowest for this region. Nevertheless, the highest was the scale parameter estimated for the inner region, and the lowest was estimated for the outer XLPE. Also, the quality of the cable peeling could influence the breakdown values. The possible influence is commented on later in subsection 4.4.

In an evaluation of the parameters found for the Weibull distribution of the DC breakdown strength in the different regions, the shape parameter must also be set in context. It can be seen that the three shape values are >1. This is expected since a shape value higher than one implies that the test object has an increasing rate of failure statistic throughout its lifetime. From an experimental perspective, the rate of failure increases with increased ramped stress. Such a development within XLPE cable insulation is well known. The biggest shape value, 6.2, is estimated for the test series performed on the middle XLPE. In addition, this corresponds with the plot in Figure 4.1, where it can be seen that the distribution giving the steepest plot is the DC breakdown values for the middle XLPE. The lowest shape value is seen for the test series of the inner XLPE, where $\beta = 3.7$. Thus, the different sizes of the shape values for the regions indicate the biggest and lowest spread in the inner and outer XLPE data sets, respectively. This observation agrees with the analysis of the 95% CIs, where the largest interval was estimated for the scale parameter of the inner XLPE, and the smallest interval was estimated for the middle XLPE.

Considering both the scale and shape values of the distributions, the highest 63.2% DC breakdown strength is estimated for the inner XLPE. However, the lowest shape value and the largest 95% CI are found for inner XLPE. Thus, the biggest spread in values could be seen for this test series. It also gives an indication of more uncertainty in the obtained values than for the tests performed on the middle and outer XLPE.

Regarding the previous studies described in subsection 2.7, the DC breakdown tests in Study 2 were conducted on unaged XLPE insulation. The report of Study 1 gives no information on the condition of the tested insulation. Therefore it is reasonable to think that the insulation did not face thermal-electrical stress before testing. The insulation may be fresh in the sense of the possibilities to produce such insulation in earlier years. However, it is reasonable to assume that the tested insulation was chemically less clean due to development within material technology and the production run of a cable.

The obtained DC breakdown strength of the aged insulation and the results from previous studies are not directly comparable. However, the DC breakdown values from the previous studies can support the reliability of the results found in this experimental work. In Study 1 from 2005, the found scale parameters of the inner and outer regions of XLPE were 440 kV/mm and 451 kV/mm, respectively. In Study 2 from 2017, DC breakdown tests were performed at different temperatures. Only the results from the tests performed at 30°C are considered. For the inner XLPE, the estimated scale parameter was $\approx$ 433 kV/mm, and for the outer XLPE, it was $\approx$ 429 kV/mm. The lowest scale parameter was found for the middle XLPE; 405 kV/mm.

It can be observed that the highest scale parameter found for the aged insulation is equal to the lowest found in the two previous studies, thus 405 kV/mm. It is expected that the breakdown values for aged insulation would be lower than for fresh insulation, thereby the obtained DC breakdown values are reasonable to consider valid. A further comparison will not be made between the aged insulation and previous studies. But, later in subsection 4.2, several aspects of the experimental work in the previous studies and this project will be commented on.

4.2 The DC breakdown strength of fresh XLPE cable peeling

In Figure 4.2 the Weibull probability plot for the DC breakdowns tests performed on the fresh cable peeling is given. Furthermore, the scale and shape parameters of the Weibull distribution for each of the DC breakdown strengths of the different regions are presented in Table 4.2. The data on the different regions follow the same indications of colors as for the plots on the aged cable peeling, but there are new markings.

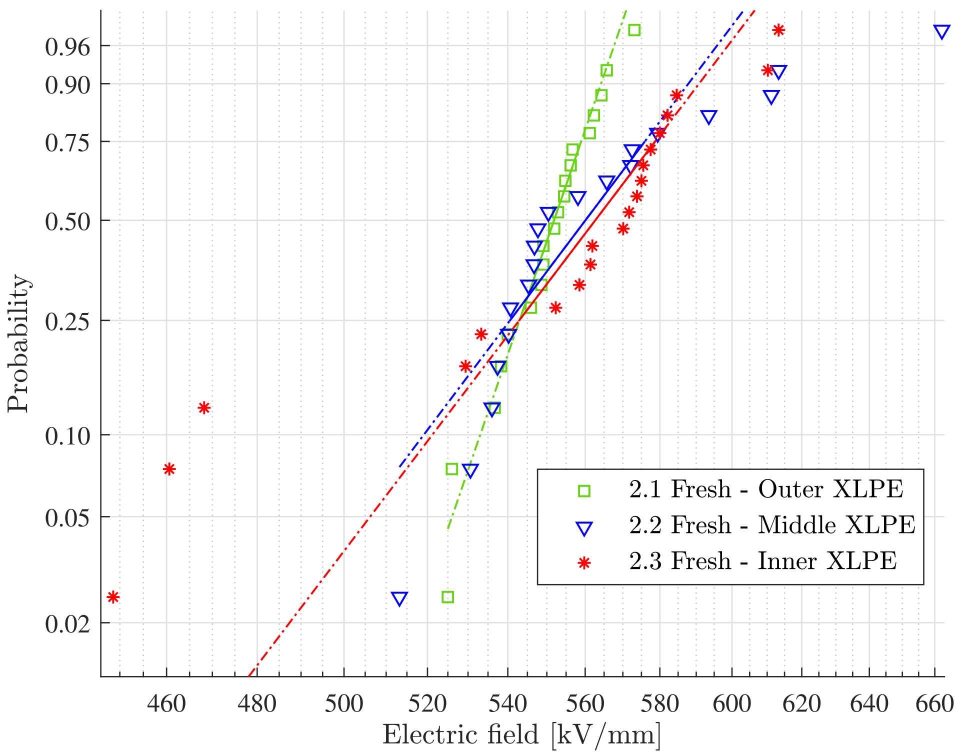

Figure 4.2: Weibull probability plot of the DC breakdown strength of the fresh XLPE insulation. Each color and type of marking indicate one region of the insulation.

Table 4.2: Scale and shape parameters of the Weibull distribution for the three test series performed on aged XLPE insulation. The 95% CIs for the values are given in cursive.

Test series/region	$\hat{\alpha}$ [kV/mm]	$\hat{\beta}$
2.1 Fresh - Outer XLPE	556 *95% CI: 551-561*	51.9 *95% CI: 37.1-72.4*
2.2 Fresh - Middle XLPE	580 *95% CI: 562-600*	14.2 *95% CI: 10.5-19.1*
2.3 Fresh - Inner XLPE	573 *95% CI: 558-587*	17.9 *95% CI: 12.5-25.7*

It can be seen from Table 4.2 that all the shape values ($\hat{\beta}$) are >1 for the Weibull distributions for the regions in the fresh cable peeling. This is not surprising as the same is expected for the fresh cable peeling as for the aged as the material is XLPE insulation; the rate of failure increases with time.

Looking at the $\hat{\alpha}$-values, the highest is given for middle XLPE, where the value is an electrical field strength of 580 kV/mm. On the other hand, the lowest value of 556 kV/mm belongs to the region of outer XLPE. The most significant difference in DC breakdown strength based on the obtained values is 24 kV/mm. The scale parameter for the inner XLPE is 573 kV/mm. This is closer to the middle XLPE value than the outer XLPE value.

Considering the 95% CIs of the calculated scale parameters, the one for the inner XLPE partly overlaps with both the CIs for the middle and outer XLPE. This indicates that there is no statistically significant difference in the 63.2% DC breakdown strength of the inner XLPE compared to the middle XLPE nor compared to the outer XLPE.

Furthermore, only considering the given 95% CIs for the outer and middle XLPE, and thereby not taking into account how the CI would look on the plot, these do not overlap. The lack of overlap can be interpreted as a significant difference in the scale parameter of the outer and middle XLPE. However, the lack of overlap is barely a fact, as the maximum limit of the outer XLPE is 561 kV/mm, and the minimum limit for the middle XLPE is 562 kV/mm. Hence, a possible significant difference is not large. Regarding the length of the CIs, these are not very diverse:

- Outer XLPE: (561 - 551) kV/mm = 10 kV/mm
- Middle XLPE: (600 - 562) kV/mm = 38 kV/mm
- Inner XLPE: (587 - 558) kV/mm = 29 kV/mm

The smallest interval, 10 kV/mm, is given for the scale parameter estimated for the regions of the outer XLPE. Furthermore, the largest interval is given for the middle XLPE, where the interval is 38 kV/mm. For the region of inner XLPE, the 95% CI range is 29 kV/mm. The given sizes of the 95% CIs indicate that the most extensive spread in the data sets can be found for the middle XLPE, while the smallest spread is in the data set of the outer XLPE. The smaller spread suggests a better fit of the 2-parameter Weibull distribution for the DC breakdown data obtained for the outer XLPE than for the middle and inner XLPE. A better fit could indicate higher reliability in the data of the outer XLPE.

Concerning the spread of the obtained DC breakdown strength values, the shape values for the different test series accord with the distinction in the size of the CIs. The lowest shape value is found for the middle XLPE; $\hat{\beta} = 14.2$. Slightly bigger, the shape value for the data set of the inner XLPE is estimated to be 17.9. The largest shape value ranges noticeably over the two others where $\hat{\beta} = 51.9$. This shape value belongs to the data set of the outer XLPE. The difference in the calculated shape values is also seen in the Weibull probability plot in Figure 4.2. It can be seen that the plot of the distribution for the outer XLPE is much steeper compared to the plots for both the middle and inner XLPE.

As there is a big difference in the shape value of the outer XLPE and the two other regions, a direct comparison of the DC breakdown strength of the different regions may be done with moderation. However, the difference in the calculated scale parameters is not of considerable size. No significant difference is found for the scale parameter of the inner XLPE relative to the middle and outer XLPE. Even though the CIs for the middle and outer XLPE do not overlap, considering the interval in number format, it could be reasonable that the plotted 95% CIs would show something different.

In Figure 4.3a and 4.3b, two examples of breakdown channels in the fresh XLPE cable peeling are shown. Figure 4.3a shows a breakdown channel where it was observed little pitting around the channel. While for the breakdown channel in Figure 4.3b, a notable amount of pitting was seen. Both figures show the irreversible destruction of the material as it is a physical hole through the peeling.

(a) A breakdown channel where it was seen a small amount of pitting.

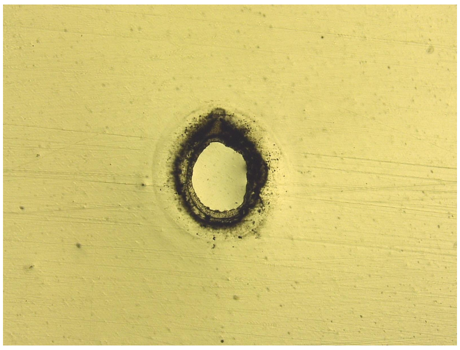

(b) A breakdown channel where it was a clear marking of pitting.

Figure 4.3: Breakdown channels from the fresh cable peeling.

In the previous studies the cable peeling was manufactured from a cable with unaged XLPE insulation. The experimental work of both studies considered the breakdown strength of the radial position of the insulation. The same form of XLPE insulation was tested. Thus, the manufacturing involved cutting the cable peeling from the outer to the inner semiconductor. The thicknesses of the cable peelings from Study 1 and Study 2 were 100 µm and 200 µm ±20 µm, respectively. However, the thickness in Study 1 is 100 µm for the whole peeling, and no evaluation of the possible variation within the peeling is highlighted. For Study 2, the thickness of 200 µm ±20 µm is based on the average value of three measurements done near the breakdown channels.

Comparing the DC breakdown strength of fresh insulation collected in this project with the ones from the previous studies, the values of this project are generally in a higher range. Regarding the tests performed in Study 2, only the ones performed at 30°C are considered. For this project, the DC breakdown strengths of the three regions are higher than 550 kV/mm. In the two previous studies, the DC breakdown strength was in the range of 400-450 kV/mm.

The difference in the determined DC breakdown strength can result from several factors. The experimental work and the geometry of both samples and electrodes will influence the obtained results. The electrode geometry in the test setup used in this project and the voltage ramping are different from the ones used in the previous studies. In the previous studies, the voltage ramping rate is faster than the step voltage profile used in this project. Due to this, it could be expected higher breakdown strength in the previous studies. However, the opposite is seen, meaning it is likely another factor making a difference in the breakdown values.

Although the test samples were XLPE cable peeling for all the studies, the peeling was cut from different types of cables. The peeling in the previous studies was from smaller cables for lower voltage levels. Consequently, the insulation layer is thinner, and the material matrix will be different from the thicker insulation layer in a 525 kV HVDC cable. In addition, the material matrix of XLPE will also vary for each cable production. The XLPE insulation tested in this project is from a 525 kV HVDC cable produced with the latest conditions and extruded in the cleanest possible manner. The higher breakdown strength could indicate that the XLPE matrix in the tested insulation in this project is better than the ones in the previous.

In addition to a difference in the material matrix, there is a difference of 100 µm in the thickness of the cable peeling between this project and Study 2. Also, the greatest difference found in obtained DC breakdown strength is between this project and Study 2. In Study 2, the largest scale parameter was ≈ 433 kV/mm, while the lowest scale parameter for fresh XLPE in this project was 556 kV/mm. The volume effect can influence electrical breakdown, and it may be this phenomenon having an influence here.

4.3 Comparison: DC Breakdown strength of Fresh vs. Aged XLPE cable peeling

Figure 4.4 shows a bar chart of the 63.2% characteristic breakdown strength of the different regions of fresh and aged cable peeling. The three bars to the left and right belong to the fresh and aged insulation specimens, respectively.

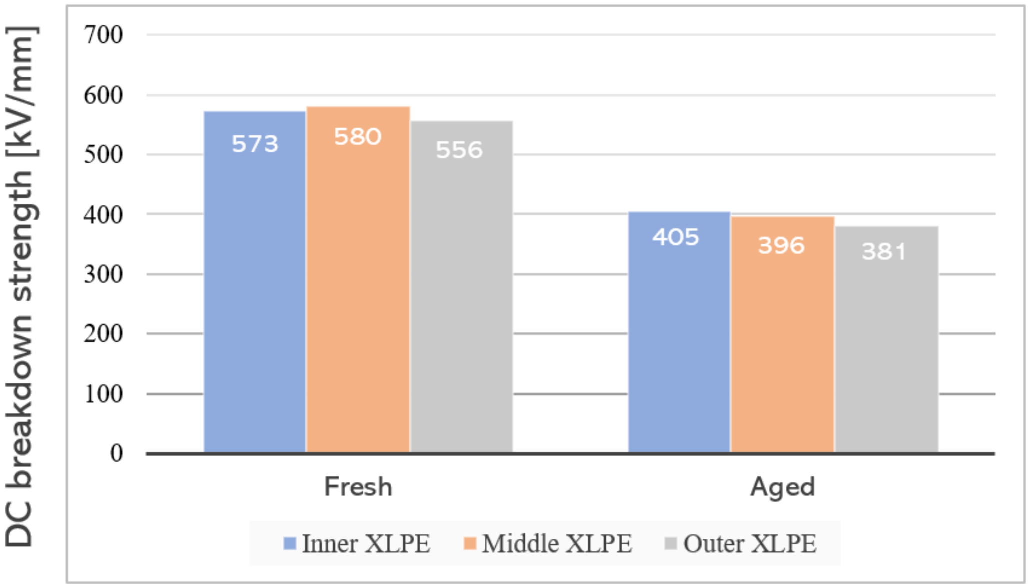

Figure 4.4: A bar chart comparing the 63.2% characteristic breakdown strength (scale parameter) of the fresh and aged XLPE cable peeling.

The bar chart in Figure 4.4 shows an evident difference in the DC breakdown strength of the regions of the fresh and aged insulation. The scale parameters of the aged specimens are more than 100 kV/mm lower than those of the fresh specimen. It is observed that for both the fresh and aged insulation, the lowest scale parameter is given for the outer XLPE. Lowest found breakdown strength for the outer XLPE could be due to the manual cutting of the cable peeling. Possible uneven cutting could lead to minor damages in the peeling; hence it could be a reason for an enhancement of a local field at even low electrical field strengths. Nevertheless, since the 95% CIs did not show a statistically significant difference in the breakdown strength of the different regions, it is reasonable that this resemblance is a coincidence.

Another similarity is the greatest difference in the scale parameter between the regions in the insulation. In the presentation of the DC breakdown strength of the different insulation specimens in subsection 4.1 and 4.2, the greatest difference was found to be 24 kV/mm. However, this difference was between the middle and outer XLPE for the fresh specimen. For the aged, it was between the inner and outer XLPE.

Although no significant difference is seen in the DC breakdown strength based on radial position in the insulation, a distinct reduction is observed when comparing the two insulation specimens. The reduction of the 63.2% characteristic breakdown strength of the fresh insulation relative to the aged insulation is given in Table 4.3.

Table 4.3: Reduction of the 63.2% breakdown strength (scale parameter) considering the fresh and aged insulation specimens.

Region	$\hat{\alpha}$ [kV/mm] Fresh insulation	$\hat{\alpha}$ [kV/mm] Aged insulation	Reduction of strength
Inner XLPE	573	405	29%
Middle XLPE	580	396	32%
Outer XLPE	556	381	31%

From both Figure 4.4 and Table 4.3, the biggest difference in scale parameter considering the regions of the two specimens is for the middle XLPE. The difference in electrical field strength is 184 kV/mm, giving a reduction of 32%. The difference in field strength of the outer and inner XLPE is 175 kV/mm and 168 kV/mm, respectively. The resulting reduction is 31% and 29%. It is a similar reduction in the scale parameters for all regions. The similar reduction suggests no difference in the breakdown strength of the regions of fresh and aged insulation. The same reduction accords with no finding of statistically significant differences within each specimen.

Reduction in DC breakdown strength is expected as the aged specimen has been through PQ tests, which intends to represent the long-term performance of a cable system. The reduction can be a natural cause from the thermo-electrical aging of the insulation. Since cable systems are designed to live at least 40 years, the PQ tests could represent these years. As the found reduction is 30% after the PQ tests, it is reasonable to suggest an even longer life of the insulation. However, if the same reduction could be expected in an actual HVDC cable is hard to consider. Nevertheless, a longer lifetime than 40 years is likely.

In addition to the scale parameters obtained for the Weibull distributions, the shape parameters must also be considered. Table 4.4 lists the estimated shape values.

Table 4.4: The shape values for the different regions of fresh and aged insulation specimens.

Region	$\hat{\beta}$ [kV/mm] Fresh insulation	$\hat{\beta}$ [kV/mm] Aged insulation
Inner XLPE	17.9	3.7
Middle XLPE	14.2	6.2
Outer XLPE	51.9	5.1

The shape values are generally lower for the test series performed on the aged cable peeling than for the fresh cable peeling. The lower shape values indicate a more extensive spread in the collected DC breakdown values for the aged insulation than for the fresh.

Considering the 95% CIs of the scale parameters, the lengths of the CIs given for the regions in the aged specimen were 70-100 kV/mm. For the regions in the fresh specimen, the interval lengths were a size of 10-40 kV/mm. The shorter lengths of CIs of the fresh insulation imply a better fit to the 2-parameter Weibull distribution. The evident difference in shape values suggests more uncertainty in the obtained data of the aged insulation. The reason for more variety in the aged cable peeling is hard to point out. The problem with destructive tests on solid dielectrics is that it is impossible to test the same material several times, unlike dielectric liquids and gases. In addition, since the tests were done on two different specimens of cable peeling, there could be more variety in the test objects. Even though it was attempted to do similar manufacturing and handling of the test objects, it will naturally be different in practice. However, the reduced shape parameter may show that aging does not occur homogeneously throughout the insulation.

The shape value of 51.9, belonging to the data obtained for the outer XLPE, clearly differs from the other shape values. The reasons for this are not obvious. The outer XLPE was the first tested region, meaning possible effects of ambient conditions can be neglected. It could be an argument against the discussion around the reason for the lowest scale parameter of the outer XLPE for both specimens. A proposed argument was that the lower breakdown strength in the outer XLPE region could result from uneven cable peeling. However, if the outer region of both cable peelings was uneven and damaged, in that case, it is reasonable to think there would be a greater spread of the breakdown values obtained here.

Comparing the results from the fresh and aged specimens of XLPE insulation, no connection between which region has the highest DC breakdown strength is seen. The only corresponding breakdown strength of the different regions is that both specimens had the lowest breakdown strength in the outer XLPE. Ranking the two other regions after the highest breakdown strength does not give the same pattern. Considering the 95% CI as well, there is no significant difference between the different regions of the insulation. The lack of overlap in the 95% CIs is an additional argument for no connection between DC breakdown strength and radial position in insulation. It is reasonable to think that it is the stochastic behavior of electrical breakdown that is observed.

In the Weibull probability plot of the DC breakdown strength of the aged and fresh XLPE insulation, in Figure 4.1 and 4.2 all the breakdown values are plotted. For the fresh insulation it is only observed four outlaying points, while for the aged insulation the spread is considerable. The form of the plot in Figure 4.1 may suggest that the breakdown data of the aged insulation fit a 3-parameter Weibull distribution better than the 2-parameter. However, this has not been tested and verified.

4.4 Possible errors/limitations in measurements

The determined values on the DC breakdown strength of the XLPE cable peeling are affected by several external factors. Throughout the experimental work, it is desired to reduce the effect of the external factors as much as possible. However, complete elimination is not possible. Therefore, in this subsection, possible errors in the measurements are considered. The commented possible errors are based on factors that could have an influence on the obtained DC breakdown values.

4.4.1 Handling/preparation of the test objects

The AC breakdown tests performed in the Specialization project experienced a notable amount of dust in the oil as the cable peeling was pulled through the test cell [1]. DC breakdown tests can be more sensitive to pollution in the oil. Therefore, cleaning the whole test sample with isopropanol was included as a point in the procedure for the DC breakdown testing. It is reasonable to think that the cable peeling still would have some dust after the cleaning. However, the worst dust particles were removed, the oil was kept clean, and the obtained DC breakdown values were in an expected range.

Another factor that could influence the DC breakdown values is the amount of moisture in the test samples. Therefore, the test objects were transported and stored in such a way that the effect of humidity on the breakdown values was reduced. However, when performing tests on each of the two cable peelings, the samples were kept in the test cell for the whole testing period. Consequently, the insulation was exposed to ambient conditions and humidity. Despite that, same as for the aspects of dust, unexpected DC breakdown values were not obtained.

In the preparation before testing, the cable peeling samples were degassed in a heating cabinet. Also, possible humidity was removed. Due to failure in planning, the aged cable peeling was only degassed for 24 hours instead of 3 days. To keep the same foundation for the test samples, the fresh and aged cable peeling were degassed for the same amount of time. As the degassing removes by-products from the crosslinking process, removes mechanical stress, and stabilizes the insulation, a short thermal treatment could affect breakdown values. The reason for stabilizing the insulation is that the results of experimental work should be reproducible, and comparison of all measurements may gain higher validity. Due to only 24 hours of thermal treatment, it is reasonable to think that the tested insulation did not have the desired condition considering reproducibility. There is some uncertainty when comparing the two tested cable peelings in this project. However, the same thermal treatment was performed for both samples. Suppose an unstable material matrix of XLPE and by-products highly influenced the breakdown values. In that case, one might expect more spread in the data sets. As this is not the case, it may be acceptable to consider the obtained results comparable. In addition, the thermal treatment in the previous studies also lasted for 24 h.

From the perspective of having the same base for the two specimens to be comparable, one may mention the problem with experimental work on solid dielectrics. Due to the irreversible destruction of the material, a new part of the material is tested for each breakdown test. In addition, when testing the fresh and aged insulation, two different cable peeling samples were used, which naturally cannot be identical. However, the fresh and aged cable peeling is collected from the same HVDC cable with the same production run. Collecting cable peelings from the same cable strengthens the work, as one can argue with a similar material matrix of XLPE in both specimens. Further, manual manufacturing of the cable peeling could contribute to more variation between the cable peelings. Comments on possible thickness variation are found later in this subsection.

4.4.2 Thickness of the cable peeling

Considering the manufacturing of cable peelings, different methods are available. The method used in this project has several strengths since manually cutting in a lathe provides automatic, slow cutting. With slow cutting, modifications in the material matrix due to heating and pressure are prevented. The automated knife feed-in provides minimal thickness variation in the peeling. Other techniques are microtomy and machining in a lathe. Microtomy provides slow cutting, but the length of the cable peeling is limited. Machining in a lathe has a higher cutting speed, consequently leading to heat development. Therefore, manual cutting in a lathe could be considered the best option. However, there will be some variation in the peelings. Therefore, to ensure higher reliability in obtained results it was performed 20 breakdown tests for each region.

In the Specialization project, the thickness measurements were done using a handheld micrometer with the ability to measure the thousandths. Yet, the thousandths were not used for the thickness values because the values would involve much uncertainty [1]. The microscope used for this experimental work was easier, providing more reliable thickness measurements even though the thousandths were considered. The thickness measurements of the cable peeling considerably influence the determined electrical field strength. Taking into account the thousandths in the measurements, the electrical field strength is more accurate than considering only the hundredths.

The thickness variation within the cable peelings could also be questioned. When performing thickness measurements of the breakdown channels on the fresh cable peeling, additional measurements were taken to assess the variation within a turn. Based on the values, variation could be seen, but this is expected as the thickness was measured considering the thousandths. Therefore, measuring the thickness of each breakdown channel is highly useful to provide high accuracy in the calculated electrical field strength.

4.4.3 Automatic Voltage adjustment

The automatic adjustment of the voltage had inequalities in the ramping for each test. Due to the variac's functionality and the disturbances in the AC signal from the lab's power distribution, achieving the same voltage profile in each test was impossible. Neither the same start voltage nor the same step size was achieved for each breakdown test. This is a weakness with the automatic voltage adjustment, as different voltage profiles lead to different stress on the insulation. If the power source had been a DC generator available for automatic adjustment one may obtain more uniform step voltage profiles.

The other option available for the adjustment of the voltage was to adjust the variac manually. However, adjusting each voltage step manually would probably not give a better voltage profile as the problems regarding the variac's functionality and the disturbances in the AC signal would still be present.

4.4.4 Pitting on electrodes

A factor experienced to be a suitable solution is the bearing ball in the HV electrode in the test cell. The breakdown tests lead to pitting on the electrodes. When the cable peeling was moved to a new spot, the bearing ball would roll randomly. Consequently, there will be pitting in a new area of the bearing ball and not the same area each time. The new area provided a smooth surface against the peeling for each test, preventing possible sharp edges. A smooth surface is desired, considering a homogeneous field distribution. The even change of bearing ball reduces the possible effect of pitting on the results. Also, regular polishing of the ground electrode was done to prevent a damaged electrode.

4.5 Anchoring the DC breakdown strength values to an actual HVDC cable

Breakdown values found in experiments are often "intrinsic" because the voltage ramping is fast and higher fields are reached in a short time. Such "intrinsic" breakdown values are higher than the one related to insulation in practical cable systems. In addition, volume effects is contributing to high DC breakdown field strengths. The cable peeling has a thickness of 100 µm, which is very thin relative to an actual XLPE insulation layer in a HV power cable often being in the range of 20 mm.

Due to the commented factors, the obtained breakdown strengths cannot be directly fitted to the breakdown strength of insulation in a cable system under operation. However, testing of different cable peeling samples can provide information on how the breakdown strength changes with changed condition of the material. The foundation of testing for each sample is aimed for keeping as identical as possible making the individual results for each of the samples comparable. As one cable peeling was made of fresh insulation and the other was insulation exposed to PQ tests reflecting 40 years of thermo-electrical aging, the change can indicate how the XLPE insulation ages.

5 Conclusion

The primary purpose of this work was to investigate to what degree the short-time DC breakdown strength in the insulation layer of HVDC cables changes as the material ages. In addition, the effect of the radial position on the short-time breakdown strength was of interest.

For the aged insulation specimen, it was found no statistically significant difference in the breakdown strength of the radial position of the insulation. Neither in the fresh (unaged) specimen was it seen significant difference. Therefore, the conclusion is that the DC breakdown strength of XLPE is not dependent on the radial position in the cable insulation.

Considering previous experimental work involving the DC breakdown strength of XLPE cable insulation, found in reference [39] and [35], unaged insulation was tested. The breakdown strength of the fresh XLPE insulation in this project is over 100 kV/mm higher than the breakdown strength of the insulation tested in the previous studies. Considering possible volume effects as minor, the higher breakdown strengths indicate that the XLPE matrix of the tested insulation in this project is better than the previously tested insulation.

From the assessment of the DC breakdown data on the fresh insulation and insulation exposed to the PQ tests, a significant change in the breakdown strength is seen. The 63.2% characteristic breakdown strength was reduced from about 550 kV/mm to around 400 kV/mm. For all three regions, the reduction was ≈30%. The observed 30% reduction in breakdown strength after 40 years of thermo-electric aging suggests that the residual lifetime of the XLPE cable insulation is even longer. Therefore, predicting 40 years lifetime of the XLPE cable insulation is conservative.

Results from experimental work will always involve uncertainty since there will be possible errors in the measurements. Nevertheless, keeping the same procedure throughout the work provides reliability to the results. The results from this work are weakened due to the short pre-thermal treatment of the test samples. Short treatment can result in unstable XLPE insulation because of residual by-products and stress. However, the foundation of testing was aimed at keeping as identical as possible, making the individual results for each of the samples comparable. The obtained data was in an expected range and is therefore considered valid.

6 Suggestions for further work

Performing a more comprehensive investigation of how the electrical properties of XLPE insulation change as the material ages is essential for better understanding the aging of XLPE under DC stress. Suggestions for relevant work are listed below.

- Perform DC breakdown tests at different temperatures since there will be a temperature gradient throughout a cable under a DC field.
- Conduct electrical tests such as space charge measurements, conductivity, and dielectric response on fresh and aged insulation. The results could be set in context with the results on the breakdown strengths to assess if any correlation could be found.
- Perform measurements providing information on the structure of XLPE insulation before and after thermo-electrical aging. The results could indicate how the XLPE material matrix changes. Measurements could be FTIR, SEM, DSC, or XRD.
- Use faster ramping on the voltage to see to what degree this affects the results on DC breakdown voltage. Faster voltage ramping enables collecting more data in a shorter time. Consequently, test series in several radial positions of the insulation could be performed, providing more insight into the condition of the whole insulation layer.
- Collect test objects exposed to different duration of thermo-electrical aging. Perform different electrical tests to see how the condition changes.

Bibliography

[1] A. K. Eilertsen, "Short-Term AC Withstand Strength of XLPE Cable Peeling," *Specialisation Project Report, Department of Electric Energy, Norwegian University of Science and Technology (NTNU)*, Trondeim, Norway, 2022.

[2] G. Chen, M. Hao, Z. Xu, A. Vaughan, J. Cao, and H. Wang, "Review of high voltage direct current cables," *CSEE Journal of Power and Energy Systems*, vol. 1, no. 2, pp. 9–21, 2015.

[3] European Commission, "Delivering the European Green Deal," 2023. [Online]. Available: https://commission.europa.eu/strategy-and-policy/priorities-2019-2024/european-green-deal/delivering-european-green-deal_en

[4] ——, "Green transition," 2023. [Online]. Available: https://reform-support.ec.europa.eu/what-we-do/green-transition_en

[5] United Nations, "Do you know all 17 sdgs?" 2023. [Online]. Available: https://sdgs.un.org/goals

[6] Buchner, A. and Schichler, U., "Review of CIGRE TB 496 regarding Prequalification Test on Extruded MVDC Cables," *No. 26 (2019): Proceedings of the 26th Nordic Insulation Symposium*, p. 1, 2019.

[7] P. Le Métayer, J. Paez, S. Touré, C. Buttay, D. Dujic, E. Lamard, and P. Dworakowski, "Break-even distance for mvdc electricity networks according to power loss criteria," in *2021 23rd European Conference on Power Electronics and Applications (EPE'21 ECCE Europe)*, 2021, pp. 1–9.

[8] P. Argaut, *Underground Cables.* Singapore: Springer Singapore, 2021, pp. 759–866. [Online]. Available: https://doi.org/10.1007/978-981-32-9938-2_10

[9] F.-B. Meng, X. Chen, C. Dai, M. Zhang, A. Paramane, L. Zheng, and Y. Tanaka, "Effect of Thermal Ageing on Physico-Chemical and Electrical Properties of EHVDC XLPE Cable Insulation," *IEEE Transactions on Dielectrics and Electrical Insulation*, vol. 28, no. 3, pp. 1012–1019, 2021.

[10] E. Ildstad, *Cable Compendium: TET4195 High Voltage Equipment.* NTNU, 2006.

[11] M. Balachandran, *Aging and Degradation Studies in Crosslinked Polyethylene (XLPE).* Singapore: Springer Singapore, 2021, pp. 189–210. [Online]. Available: https://doi.org/10.1007/978-981-16-0514-7_8

[12] International Electrotechnical Commission, "IEC 62067 Power cables with extruded insulation and their accessories for rated voltages above 150 kV (Um = 170 kV) up to 500 kV (Um = 550 kV) – Test methods and requirements," p. 8, 2011.

[13] S. S. Sengupta, *XLPE Manufacturing Processes.* Singapore: Springer Singapore, 2021, pp. 41–66. [Online]. Available: https://doi.org/10.1007/978-981-16-0514-7_3

[14] K. Aljoumaa and A. W. Allaf, *Morphology, Structure, Properties and Applications of XLPE.* Singapore: Springer Singapore, 2021, pp. 125–166. [Online]. Available: https://doi.org/10.1007/978-981-16-0514-7_6

[15] E. Ildstad, *Compendium: TET4160 Insulating Materials for High Voltage Application.* NTNU, 2021.

[16] A. Barlow, "The Chemistry of Polyethylene Insulation," *IEEE Electrical Insulation Magazine*, vol. 7, no. 1, pp. 8–19, 1991.

[17] G. Chen and A. Davies, "The influence of defects on the short-term breakdown characteristics and long-term dc performance of ldpe insulation," *IEEE Transactions on Dielectrics and Electrical Insulation*, vol. 7, no. 3, pp. 401–407, 2000.

[18] J. Thomas, M. E. Thomas, and S. Thomas, *Crosslinked Polyethylene: State-of-the-Art and New Challenges.* Singapore: Springer Singapore, 2021, pp. 1–15. [Online]. Available: https://doi.org/10.1007/978-981-16-0514-7_1

[19] I. Pleşa, P. V. Noţingher, C. Stancu, F. Wiesbrock, and S. Schlögl, "Polyethylene Nanocomposites for Power Cable Insulations," *Polymers*, vol. 11, no. 1, 2019. [Online]. Available: https://www.mdpi.com/2073-4360/11/1/24

[20] A. Paajanen, J. Vaari, and T. Verho, "Crystallization of cross-linked polyethylene by molecular dynamics simulation," *Polymer*, vol. 171, pp. 80–86, 2019. [Online]. Available: https://www.sciencedirect.com/science/article/pii/S0032386119302642

[21] J. Densley, "Ageing Mechanisms and Diagnostics for Power Cables - An Overview," *IEEE Electrical Insulation Magazine*, vol. 17, p. 15, 2001.

[22] International Electrotechnical Commission, "IEC 60505 Evaluation and qualification of electrical insulation systems," pp. 13–14, 2011.

[23] J. C. Fothergill, "Ageing, space charge and nanodielectrics: Ten things we don't know about dielectrics," in *2007 IEEE International Conference on Solid Dielectrics*, 2007, pp. 1–10.

[24] L. A. Dissado and J. C. Fothergill, *Electrical Degradation and Breakdown in Polymers*, 1st ed. The Institution of Engineering and Technology, 1992.

[25] C. Jörgens and M. Clemens, "Fast calculation of steady-state charge distribution in high voltage power cables," *International Journal of Numerical Modelling: Electronic Networks, Devices and Fields*, vol. 33, no. 5, p. e2713, 2020. [Online]. Available: https://onlinelibrary.wiley.com/doi/abs/10.1002/jnm.2713

[26] T. Andrews, R. N. Hampton, A. Smedberg, D. Wald, V. Waschk, and W. Weissenberg, "The role of degassing in XLPE power cable manufacture," *IEEE Electrical Insulation Magazine*, vol. 22, no. 6, pp. 5–16, 2006.

[27] Z. Yan, K. Yang, Y. Zhang, W. S., and J. Li, "Crosslinking dependence of trap distribution and breakdown performance of crosslinked polyethylene," *Materials Science: Materials in Electronics*, vol. 30, 2019.

[28] Y. Sekii and T. Maeno, "Generation and Dissipation of Negative Heterocharges in XLPE and EPR," *IEEE Transactions on Dielectrics and Electrical Insulation*, vol. 16, no. 3, pp. 668–675, 2009.

[29] L. Dissado, J. Fothergill, A. See, G. Stevens, L. Markey, C. Laurent, G. Teyssedre, U. Nilsson, G. Platbrood, and G. Montanari, "Characterizing HV XLPE cables by electrical, chemical and microstructural measurements on cable peeling: effects of surface roughness, thermal treatment and peeling location," in *2000 Annual Report Conference on Electrical Insulation and Dielectric Phenomena (Cat. No.00CH37132)*, vol. 1, 2000, pp. 136–140 vol.1.

[30] M. Fu, G. Chen, L. A. Dissado, and J. C. Fothergill, "Influence of thermal treatment and residues on space charge accumulation in XLPE for DC power cable application," *IEEE Transactions on Dielectrics and Electrical Insulation*, vol. 14, no. 1, pp. 53–64, 2007.

[31] T. Mizutani, "Space charge measurement techniques and space charge in polyethylene," *IEEE Transactions on Dielectrics and Electrical Insulation*, vol. 1, no. 5, pp. 923–933, 1994.

[32] Cigre, "Recommendations for testing DC extruded cable systems for power transmission at a rated voltage up to and including 800 kV," *TECHNICAL BROCHURE, B1 Insulated cables, 852*, 2021.

[33] W. Hauschild and W. Mosch, *Statistical Techniques for High-Voltage Engineering.* The Institution of Engineering and Technology, IET Power Series Vol 13, 1992.

[34] H. Gupta and S. Das, "Statistical analysis of oil insualtion breakdown voltage," *2017 IEEE International Conference on Industrial Engineering and Engineering Management (IEEM)*, p. 5, 2017.

[35] X. Liu, Q. Yu, M. Liu, Y. Li, L. Zhong, M. Fu, and S. Hou, "DC electrical breakdown dependence on the radial position of specimens within HVDC XLPE cable insulation," *IEEE Transactions on Dielectrics and Electrical Insulation*, vol. 24, no. 3, pp. 1476–1484, 2017.

[36] ReliaSoft, "Characteristics of the Weibull Distribution," 2002. [Online]. Available: https://www.weibull.com/hotwire/issue14/relbasics14.htm

[37] K. Wang, F. Hsu, and P. Liu, "Modeling the bathtub shape hazard rate function in terms of reliability," *Reliability Engineering and System Safety*, vol. 75, no. 3, pp. 397–406, 2002. [Online]. Available: https://www.sciencedirect.com/science/article/pii/S0951832001001247

[38] V. Lysne and T. Olsen, "Konfidensinterller - hva kan de fortelle deg?" *Norsk tidsskrift for ernæring*, vol. 15, no. 1, 2017. [Online]. Available: https://www.idunn.no/doi/10.18261/ntfe.15.1.5

[39] N. Zebouchi, P. Carstensen, A. Farkas, A. Campus, and U. Nilsson, "Electric characterization of films peeled from the insulation of extruded hvdc cables," in *CEIDP '05. 2005 Annual Report Conference on Electrical Insulation and Dielectric Phenomena, 2005.*, 2005, pp. 79–82.

[40] Solvay, "Galden® PFPE," 2023. [Online]. Available: https://www.solvay.com/en/brands/galden-pfpe

[41] Ensinger, "POM - Acetal Polyoxymethylene ," 2023. [Online]. Available: https://www.ensingerplastics.com/en/shapes/engineering-plastics/pom-acetal

Appendix

A List of Equipment

Table A.1: Equipment used in the experimental work

Category	Equipment	Registration number
Test setup HV side	Transformer 220V/100 kV	B01-0014
	High voltage rectifier	B02-0253
	High voltage capacitor	K03-0200
	Voltage divider	I06-0471
	High voltage resistor 2.4 kΩ	K01-0484
	Earth breaker	C06-0170
	Water resistor	K01-0507
	Test cell	-
Test setup LV side	Variable AC Power Supply	B01-0555
	NI RiO module	P08-0494
	CHASSIS 4 SLOT	P08-0512
	NI cRIO module	P08-0682
	Voltage differential probe	I06-0358
	Computer	P07-3110
	Oscilloscope 2.5 GS/S	G04-0409
	Multimeter	S03-0482
	Multimeter	S03-0540
Other	Temp./humidity meter	NO7-0171

B DC breakdown data - Aged XLPE cable peeling

Table B.1: The DC breakdown data obtained for the outer XLPE of the aged specimen

DC breakdown voltage [kV]	Thickness breakdown channel [mm]	DC breakdown strength [kV/mm]
58.1	0.108	538.0
37.2	0.097	383.5
33.0	0.111	297.3
29.3	0.100	293.0
31.4	0.105	299.0
37.4	0.101	370.3
38.1	0.113	337.2
42.5	0.097	438.1
50.1	0.109	459.6
36.0	0.105	342.9
30.4	0.108	281.5
30.3	0.101	300.0
35.2	0.112	314.3
36.2	0.102	354.9
38.6	0.105	367.6
44.3	0.104	426.0
39.3	0.112	350.9
32.0	0.104	307.7
29.9	0.109	274.3
34.2	0.108	316.7

Table B.2: The DC breakdown data obtained for the middle XLPE of the aged specimen

DC breakdown voltage [kV]	**Thickness breakdown channel [mm]**	**DC breakdown strength [kV/mm]**
39.2	0.106	369.8
34.5	0.108	319.4
34.1	0.104	327.9
37.8	0.112	337.5
30.1	0.103	292.2
44.0	0.104	423.1
50.1	0.103	486.4
41.2	0.110	374.5
36.3	0.102	355.9
34.6	0.109	317.4
38.3	0.107	357.9
35.3	0.106	333.0
40.3	0.107	376.6
39.5	0.108	365.7
39.00	0.102	382.4
30.5	0.104	293.3
41.9	0.107	391.6
57.1	0.110	519.1
36.1	0.099	364.6
48.2	0.112	430.4

Table B.3: The DC breakdown data obtained for the inner XLPE of the aged specimen

DC breakdown voltage [kV]	**Thickness breakdown channel [mm]**	**DC breakdown strength [kV/mm]**
43.4	0.112	387.5
38.1	0.113	337.2
31.2	0.105	297.1
35.3	0.112	315.2
29.2	0.106	275.5
65.9	0.112	588.4
43.2	0.109	396.3
37.1	0.105	353.3
62.3	0.110	566.4
59.5	0.104	572.1
34.3	0.109	314.7
25.8	0.100	258.0
50.2	0.118	425.4
38.4	0.106	362.3
40.3	0.106	380.2
39.3	0.104	377.9
30.2	0.102	296.1
32.2	0.112	287.5
29.3	0.103	284.5
29.1	0.110	264.5

C DC breakdown data - Fresh XLPE cable peeling

Table C.1: The DC breakdown data obtained for the outer XLPE of the fresh specimen

DC breakdown voltage [kV]	Thickness breakdown channel [mm]	DC breakdown strength [kV/mm]
57.4	0.104	551.9
59.6	0.106	562.3
63.2	0.112	564.3
59.3	0.108	549.1
57.8	0.103	561.2
59.4	0.110	540.0
58.7	0.107	548.6
57.6	0.107	538.3
59.4	0.105	565.7
62.1	0.112	554.5
57.5	0.104	552.9
58.4	0.105	556.2
61.9	0.108	573.1
57.7	0.104	554.8
58.5	0.109	536.7
56.7	0.108	525.0
54.7	0.104	526.0
58.2	0.106	549.1
60.6	0.111	545.9
57.9	0.104	556.7

Table C.2: The DC breakdown data obtained for the middle XLPE of the fresh specimen

DC breakdown voltage [kV]	**Thickness breakdown channel [mm]**	**DC breakdown strength [kV/mm]**
57.3	0.108	530.6
57.5	0.107	537.4
63.5	0.111	572.1
58.6	0.105	558.1
59.6	0.109	546.8
54.4	0.106	513.2
58.4	0.108	540.7
53.6	0.100	536.0
63.3	0.115	550.4
58.4	0.102	572.5
58.5	0.107	546.7
57.8	0.106	545.3
60.5	0.112	540.2
64.9	0.098	662.2
65.4	0.107	611.2
59.1	0.102	579.4
61.1	0.108	565.7
60.8	0.111	547.7
64.4	0.105	613.3
64.1	0.108	593.5

Table C.3: The DC breakdown data obtained for the inner XLPE of the fresh specimen

DC breakdown voltage [kV]	**Thickness breakdown channel [mm]**	**DC breakdown strength [kV/mm]**
50.1	0.107	468.2
50.2	0.109	460.6
56	0.105	533.3
57.7	0.109	529.4
48	0.107	448.6
60.2	0.109	552.3
59.2	0.106	558.5
59	0.105	561.9
60.6	0.106	571.7
61.0	0.107	570.1
61.4	0.107	573.8
61.7	0.106	582.1
62.1	0.108	575.0
58.9	0.102	577.5
64	0.114	561.4
60.8	0.104	584.6
61.0	0.106	575.5
63.8	0.110	580.0
65.9	0.108	610.2
64.4	0.105	613.3

NTNU
Norwegian University of
Science and Technology